



Ruđer
Bošković
Institute

Exploring the interstellar medium and magnetic fields of the Milky Way at low-radio frequencies

Vibor Jelić

RBI - Department of Experimental Physics
Laboratory for Astroparticle Physics and Astrophysics



Ruđer
Bošković
Institute



Andrea Bracco
MSCA Postdoc @ RBI
(2020 - 2022)



Lana Ceraj
Postdoc @ RBI
(2020 - 2022)



Ana Erceg
PhD student @ RBI
(2019 - present)



Luka Turić
PhD student @ RBI
(2019 - 2023)



Iva Šnidarić
PhD student @ RBI
(2020 - 2023)



Lovorka Gajović
MSc student@UniZg
(2021)

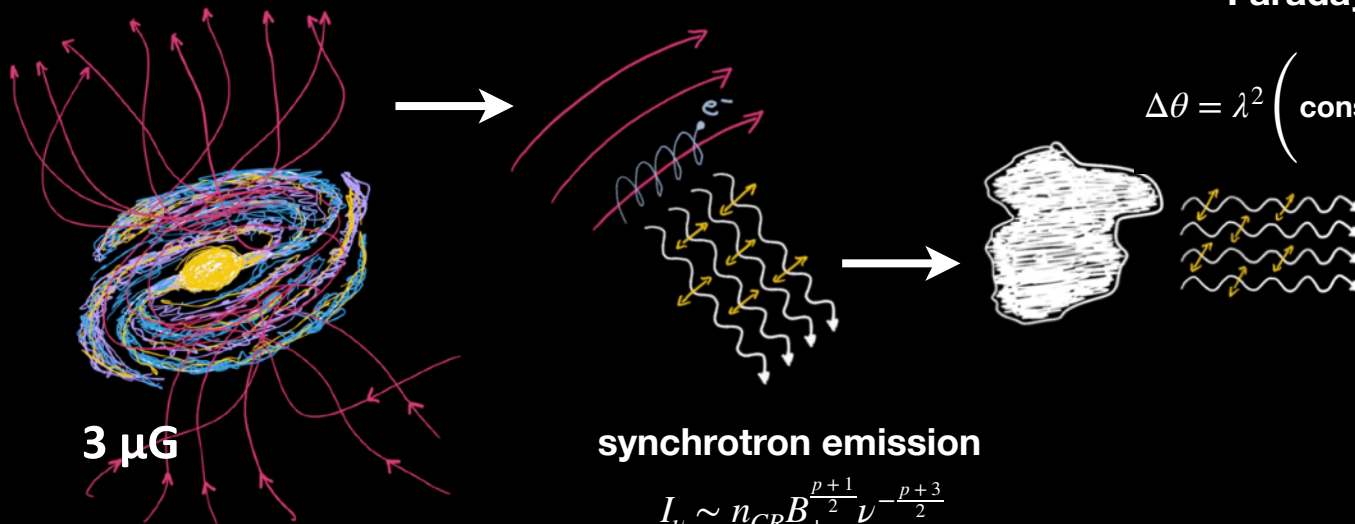


Barbara Šiljeg
MSc student@UniZg
(2021)

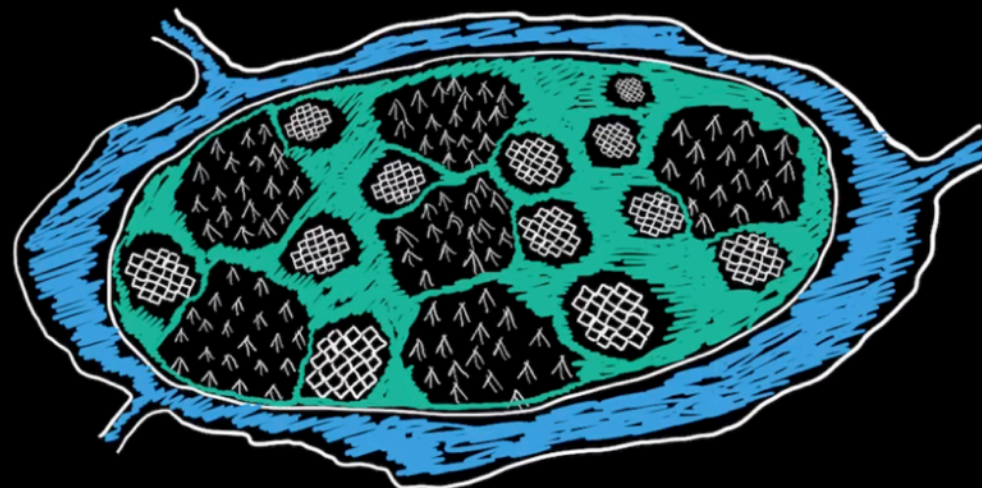
+ LOFAR Survey, Magnetism and EoR KSP teams

Faraday rotation

$$\Delta\theta = \lambda^2 \left(\text{const.} \int_0^d n_e \mathbf{B} \cdot d\mathbf{l} \right)$$



$$I_\nu \sim n_{CR} B_{\perp}^{\frac{p+1}{2}} \nu^{-\frac{p+3}{2}}$$



The Low Frequency Array (LOFAR)

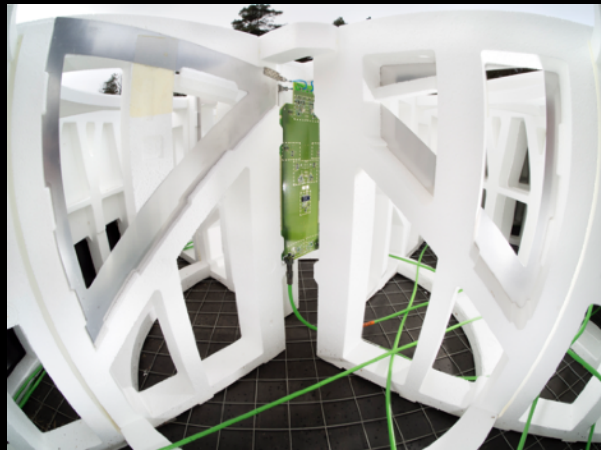
van Haarlem et al. 2013

10 - 240 MHz

LOFAR

Low Frequency Array

HBA: High Band Antenna
100–250 MHz



LBA: Low Band Antenna
10–80 MHz

LOFAR

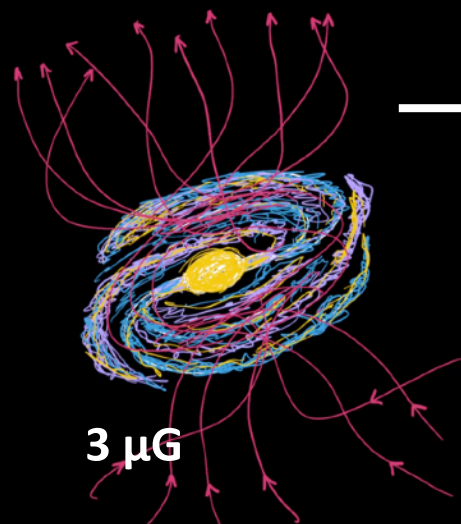
Low Frequency Array



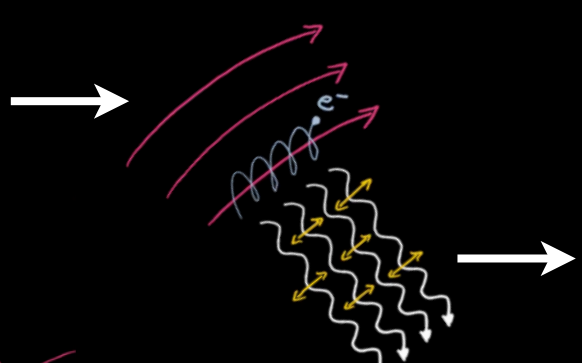
LOFAR

Low Frequency Array





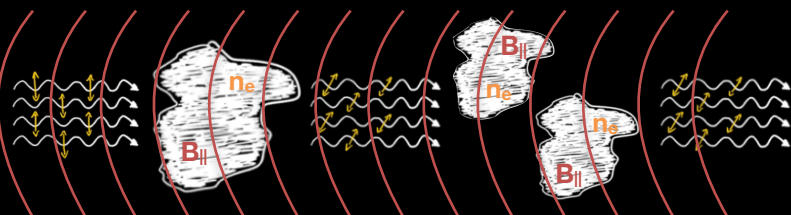
$3 \mu\text{G}$



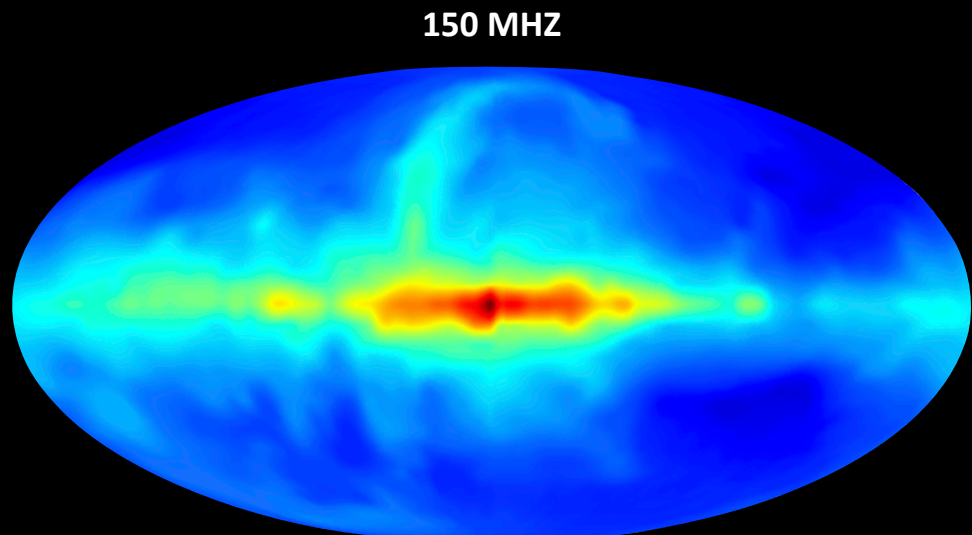
synchrotron emission

Faraday rotation

$$\Delta\theta = \lambda^2 \left(\text{const.} \int_0^d n_e \mathbf{B} \cdot d\mathbf{l} \right)$$



DEPOLARIZATION

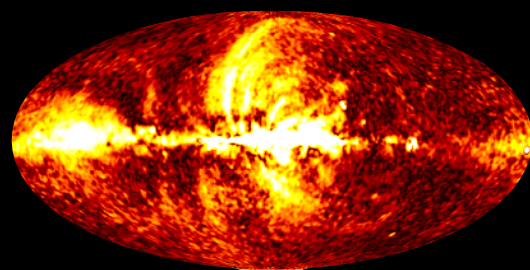


150 MHZ

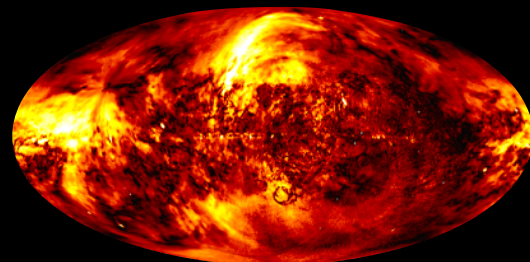
100 K

7200 K

Landecker & Wielebinski 1970



Polarized intensity @ 22.8 GHz



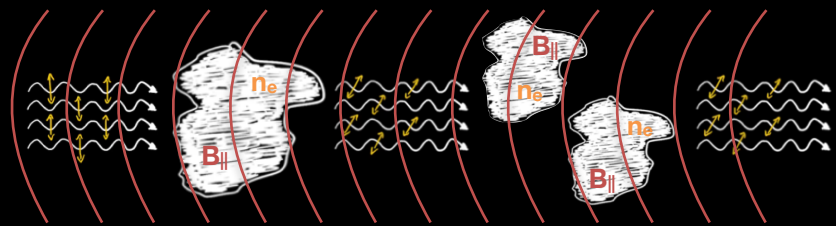
Polarized intensity @ 1.4 GHz

LINEAR POLARIZATION

Stokes Q, U

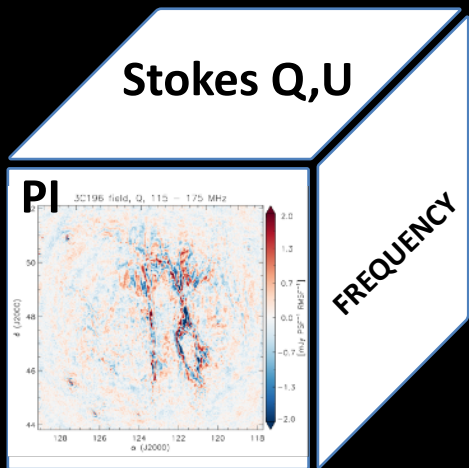
$$Q = PI \cos \theta \quad PI = \sqrt{Q^2 + U^2}$$

$$U = PI \sin \theta \quad \theta = \frac{1}{2} \tan^{-1} \frac{U}{Q}$$



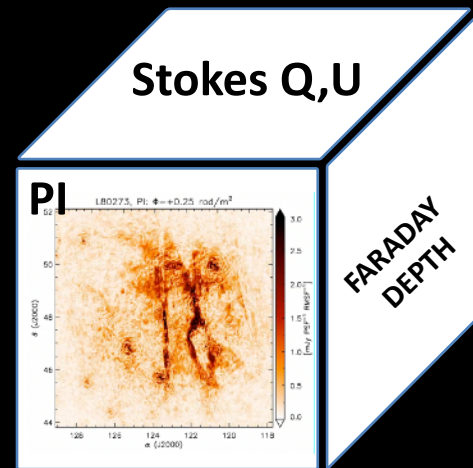
$$\theta = \theta_0 + \lambda^2 \left(\text{const.} \int_0^d n_e \mathbf{B} \cdot d\mathbf{l} \right)$$

FARADAY DEPTH



RM synthesis

Burn et al. 1966
Brentjens & de Bruyn 2008



$$\mathbf{P}(\lambda^2) = \mathbf{Q}(\lambda^2) + i\mathbf{U}(\lambda^2)$$

$$F(\Phi) = \int_{-\infty}^{+\infty} W(\lambda^2) P(\lambda^2) e^{-i2\Phi\lambda^2} d\lambda^2$$

RM synthesis

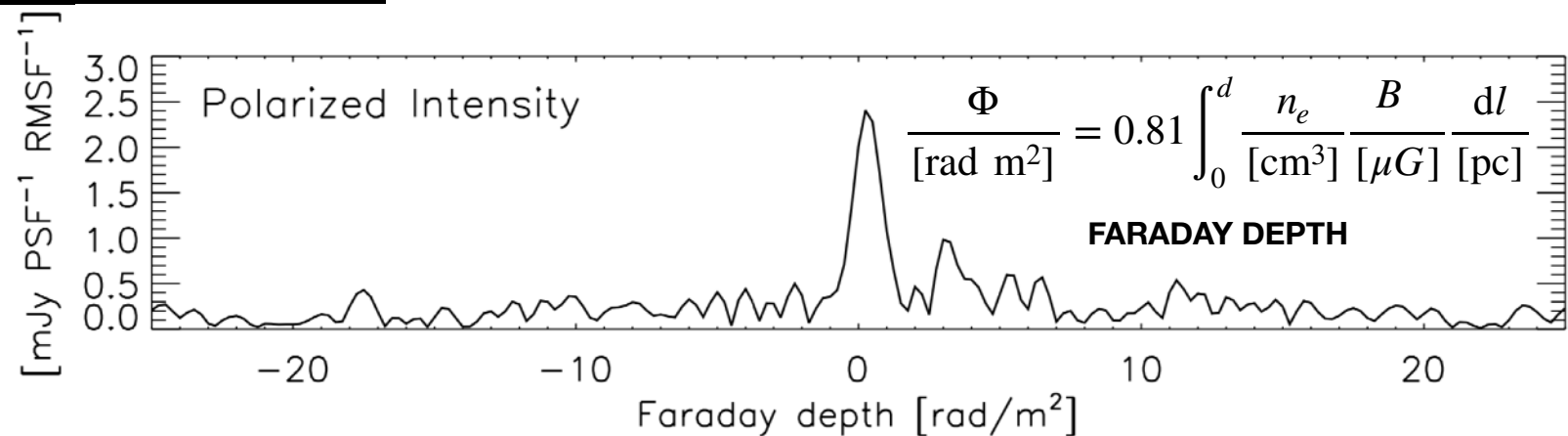
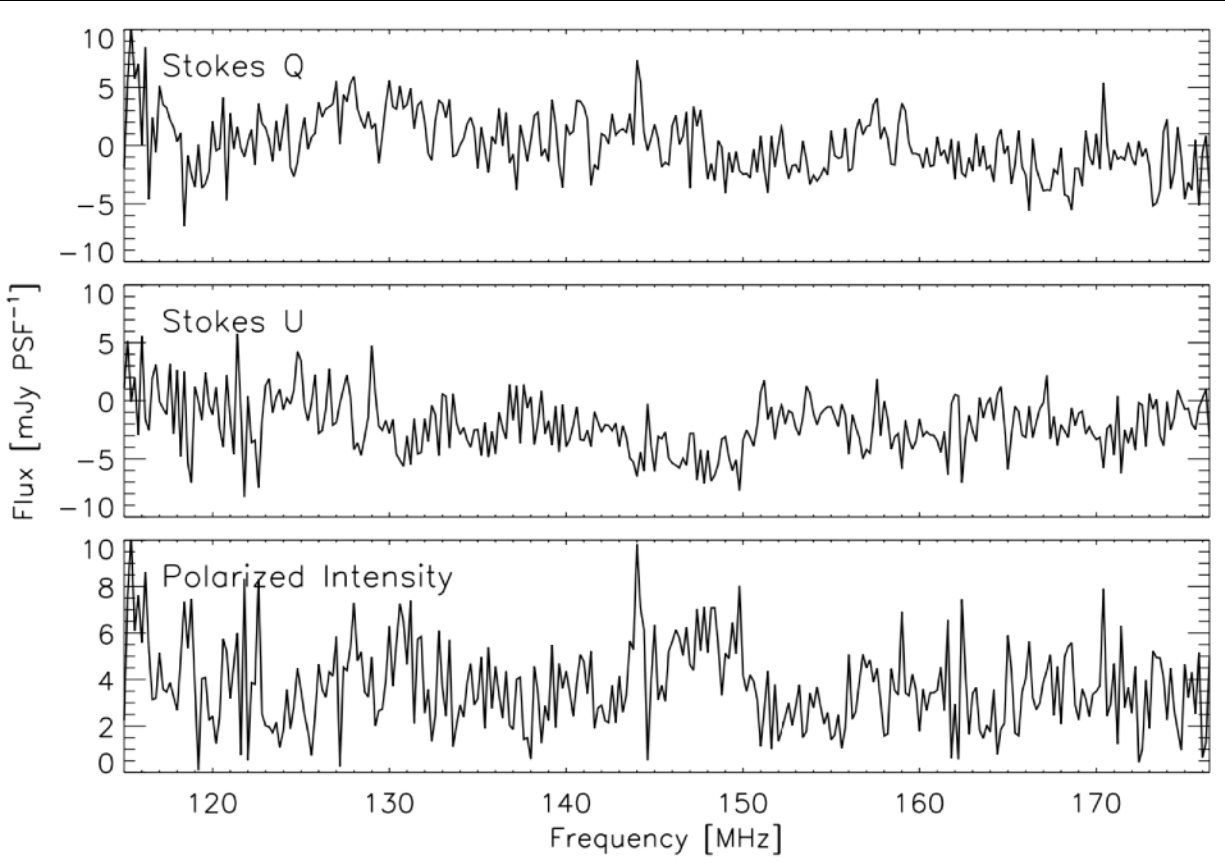
Brentjens & de Bruyn 2008

$Q(\nu), U(\nu)$

$$\mathbf{P}(\lambda^2) = \mathbf{Q}(\lambda^2) + i\mathbf{U}(\lambda^2)$$

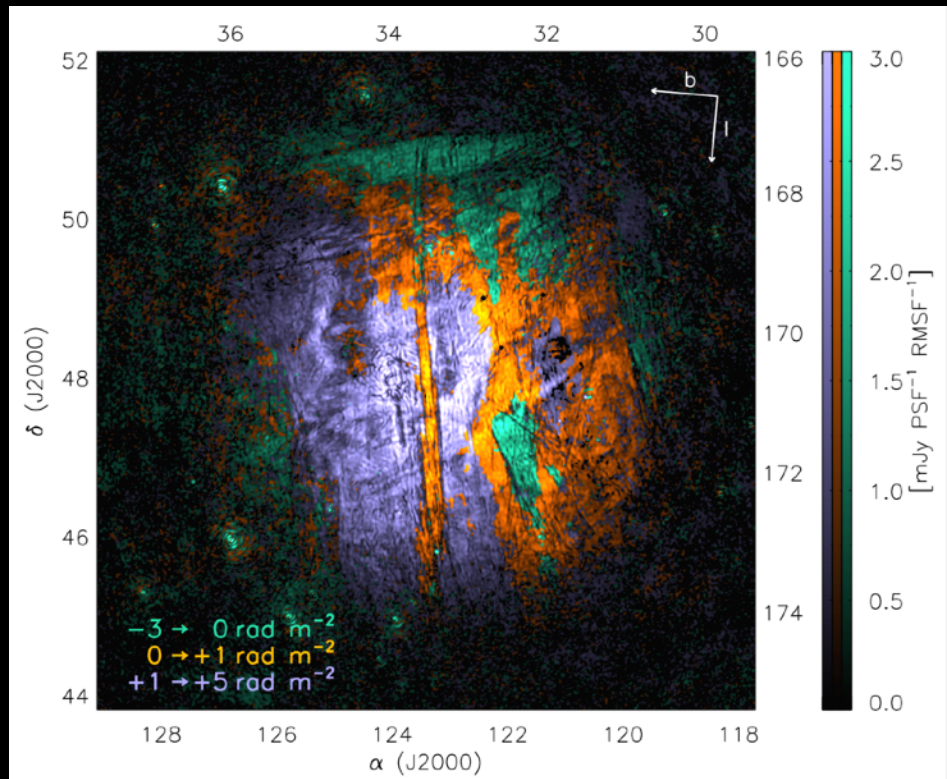
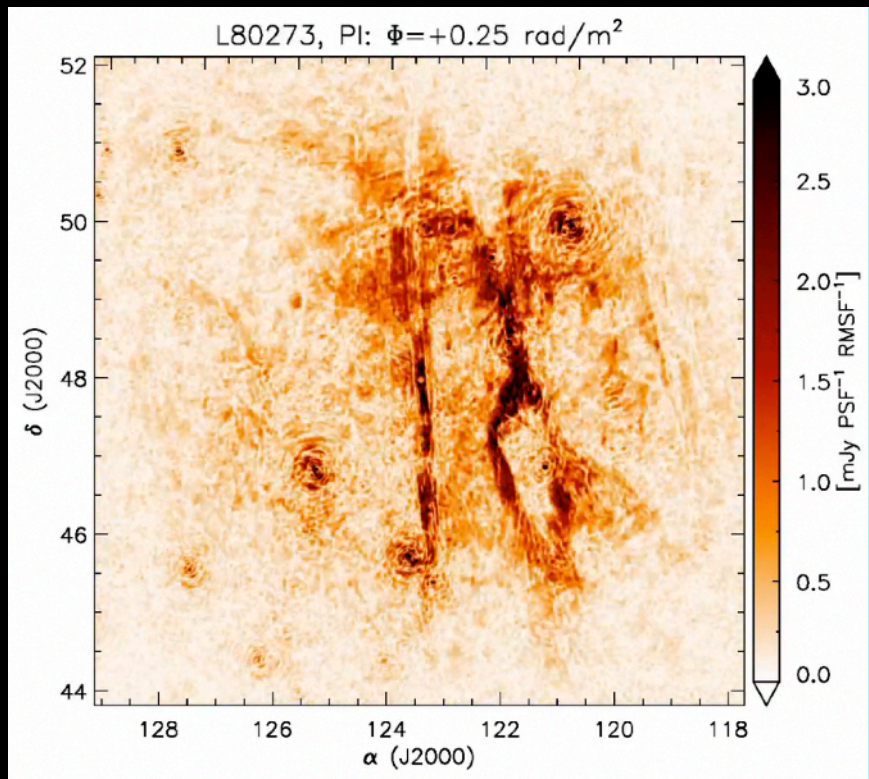
$$F(\Phi) = \int_{-\infty}^{+\infty} W(\lambda^2) P(\lambda^2) e^{-i2\Phi\lambda^2} d\lambda^2$$

$Q(\Phi), U(\Phi)$



Faraday tomography

LOFAR-HBA observations
3C 196 field
6-8 h (115 - 175 MHz, 183 kHz)
 $\delta\Phi = 1 \text{ rad/m}^2$



Jelić et al. 2015

RM synthesis

Brentjens & de Bruyn 2008

RESOLUTION IN FARADAY DEPTH $\delta\Phi \approx \frac{2\sqrt{3}}{\Delta\lambda^2}$

$\delta\Phi$ @ 150 MHz: 1 rad/m²

$\delta\Phi$ @ 350 MHz: 10 rad/m²

$\delta\Phi$ @ GHz: > 100 rad/m²

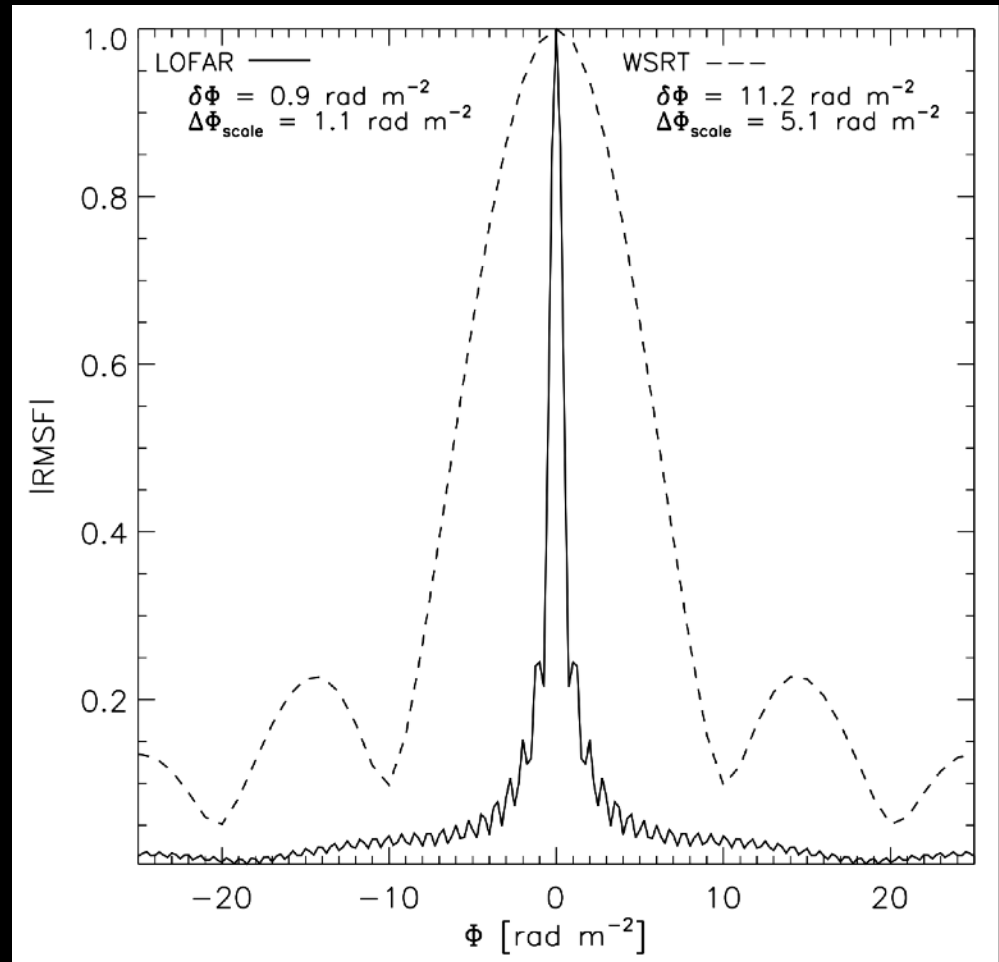
LARGEST SCALE IN FARADAY DEPTH $\Delta\Phi_{\text{scale}} \approx \frac{\pi}{\Delta\lambda^2_{\min}}$

$$\lambda^2\Delta\Phi \ll 1$$

FARADAY THIN STRUCTURE

$$\lambda^2\Delta\Phi \gg 1$$

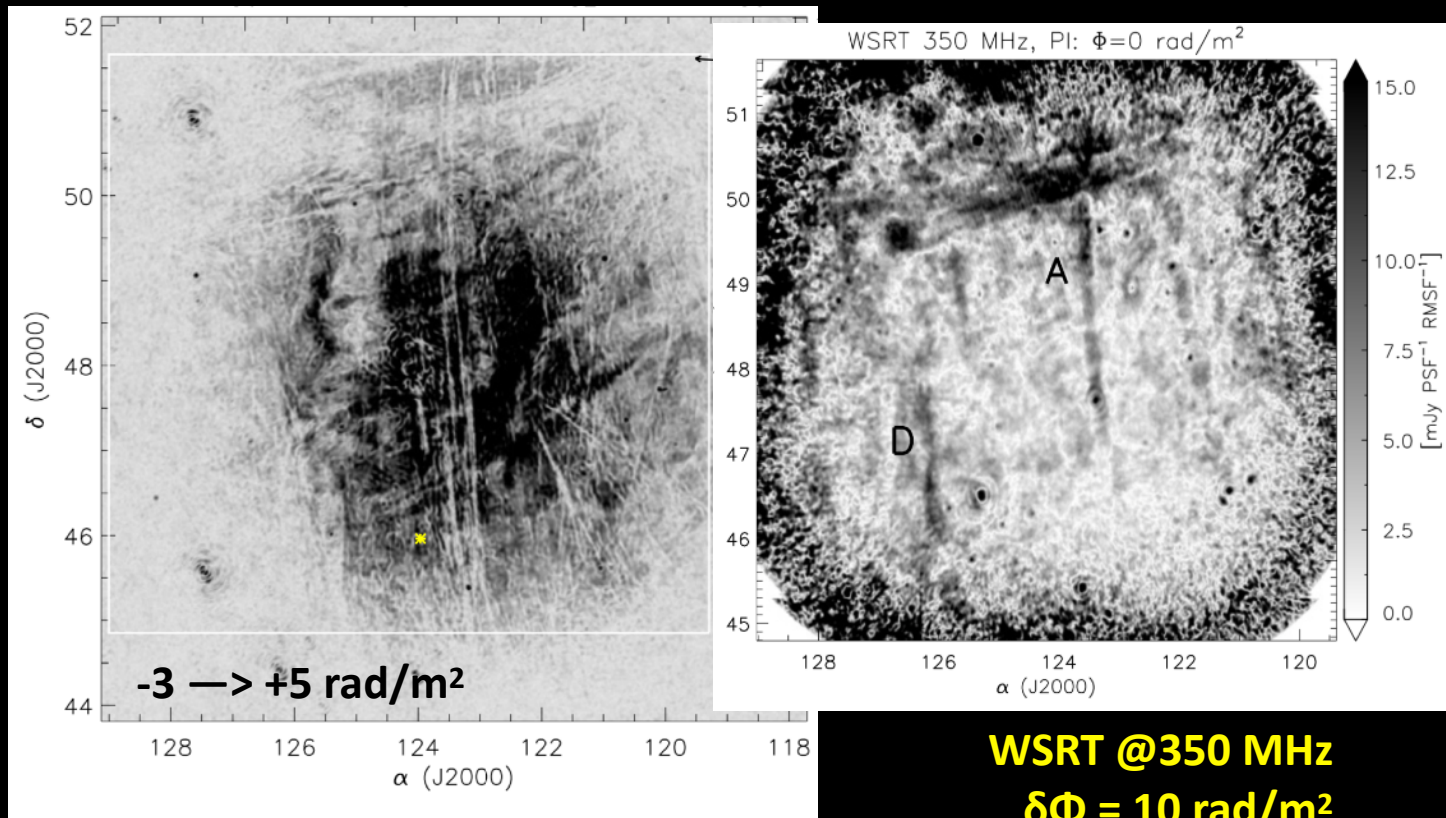
FARADAY THICK STRUCTURE



- Faraday thickness is frequency dependant, to resolve Faraday thick structure $\lambda_{\min}^2 \ll \Delta\lambda$
- observations at low-radio frequencies is sensitive to Faraday rotation caused by small column density medium

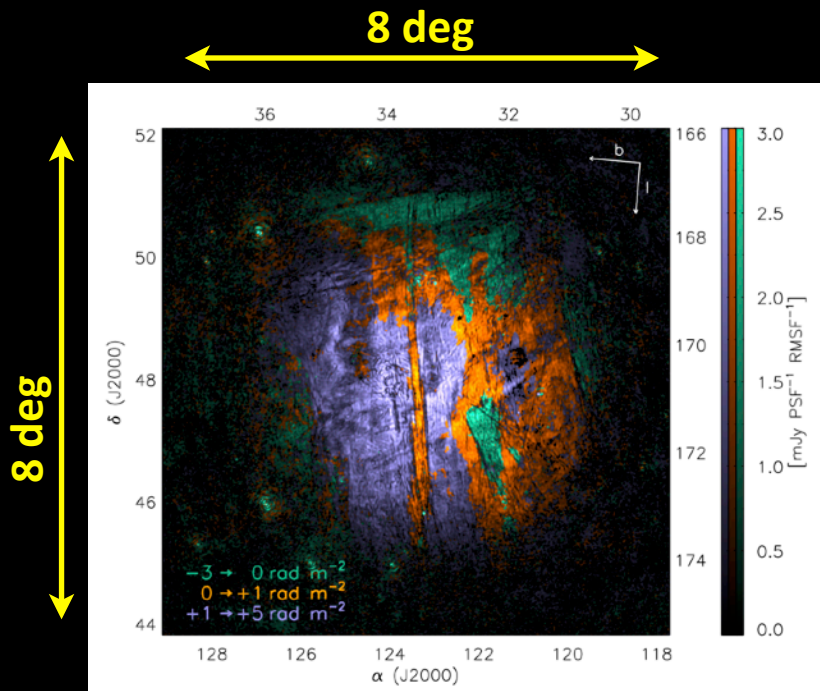
LOFAR @ 145 MHz
 $\delta\Phi = 1 \text{ rad/m}^2$

3C 196 field

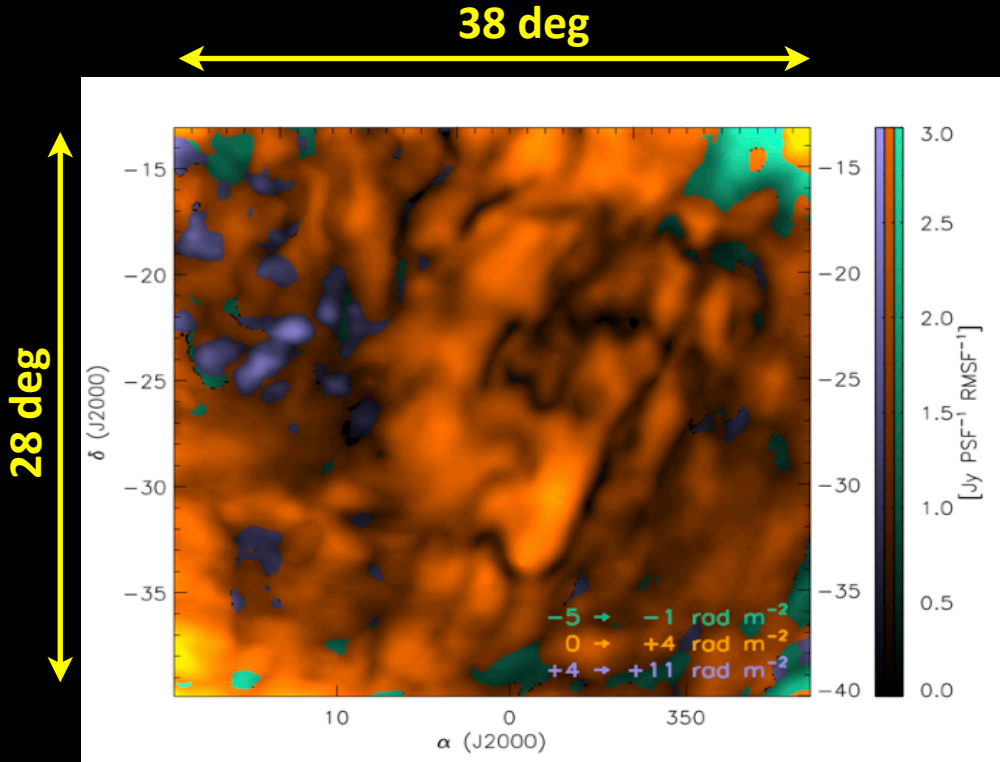


- comparable angular resolution (~3 arcmin)
- different resolution in Faraday depth (~1 rad/m² vs. ~10 rad/m²)

Faraday thin structure @ 350 MHz is Faraday thick @ 150 MHz
Jelić et al. 2015



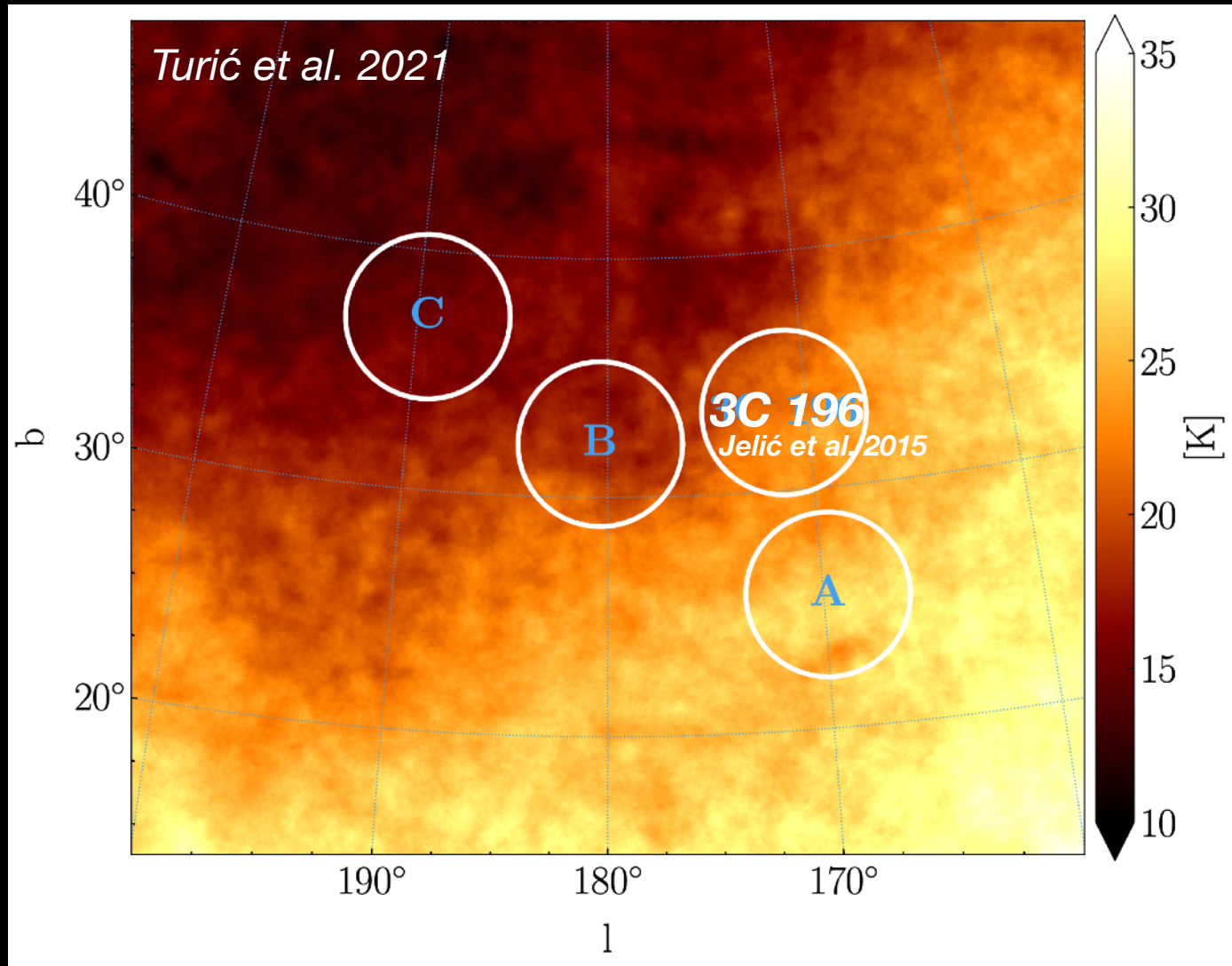
Jelic et al. 2015
LOFAR observations



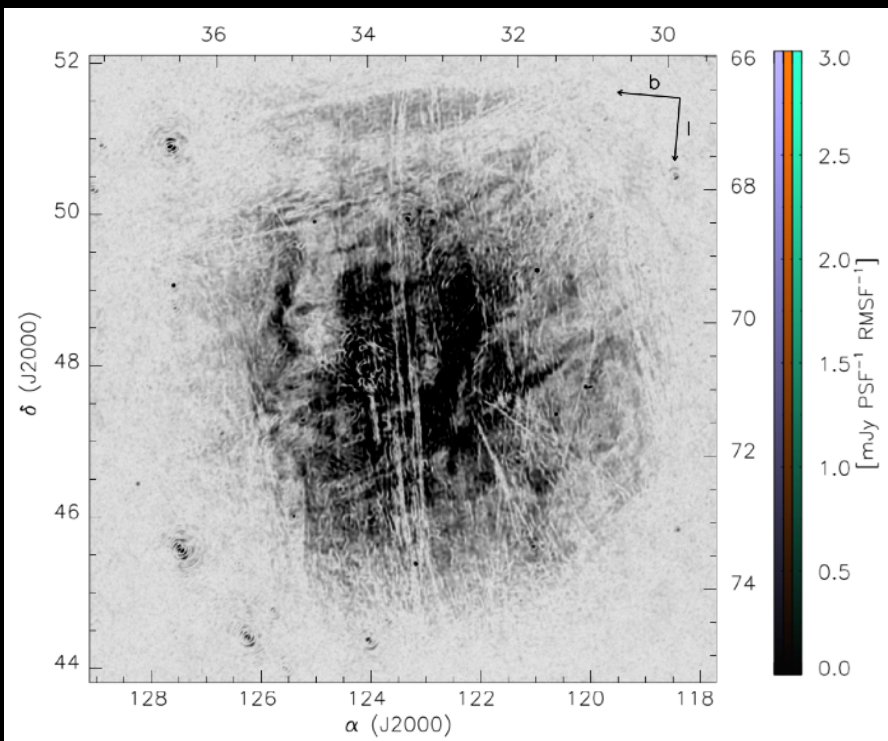
Lenc et al. 2016
MWA observations

- comparable resolution in Faraday depth ($\sim 1 \text{ rad/m}^2$)
- different angular resolution ($\sim 3 \text{ arcmin}$ vs. 1 deg)

Faraday tomography

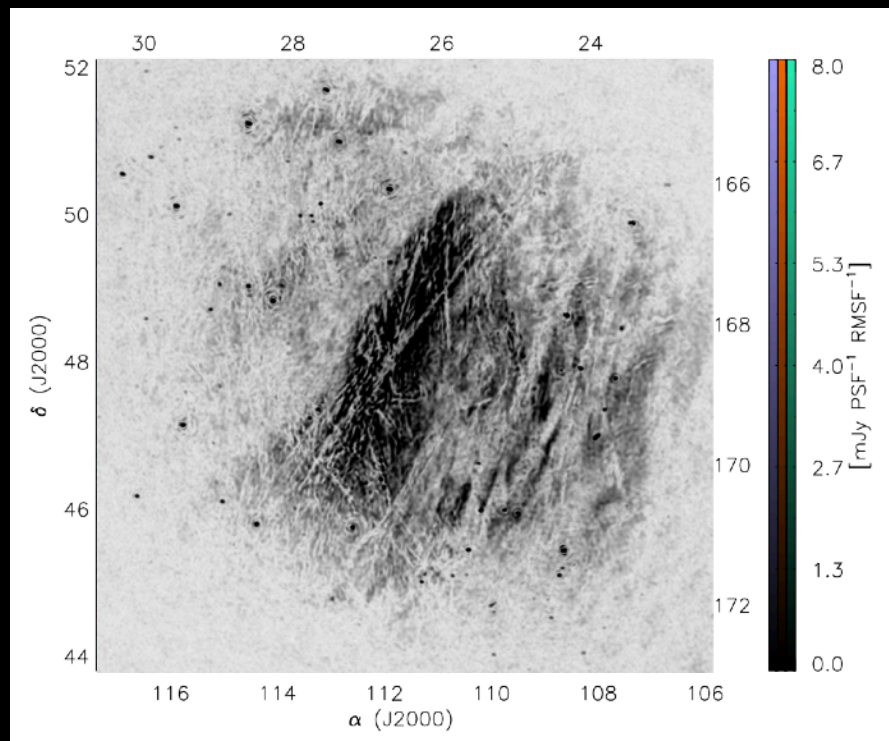


3C 196 field



Jelić et al. 2015

Field A



Truić et al. 2021

- brightness of the emission is 1-10K, only a few percent of intrinsically polarized emission

Where along the line-of-sight does depolarization happen ?

From where does the observed emission originate from ?

What drives the morphology of observed emission ?

MAGNETIC FIELDS

NEUTRAL (atomic and
molecular) or IONISED GAS
+DUST

MAGNETIC FIELDS

INTERSTELLAR MEDIUM (ISM)

Hot Ionised Medium (HIM) $T \sim 10^6$ K; $n \sim 10^{-2}$ cm $^{-3}$

Warm Ionised Medium (WIM) $T \sim 5 \times 10^3$ K; $n \sim 0.5 - 2$ cm $^{-3}$

Warm Neutral Medium (WNM) $T \sim 5 \times 10^3$ K; $n \sim 0.5 - 2$ cm $^{-3}$

Cold Neutral Medium (CNM) $T \sim 10^2$ K; $n \sim 10^2$ cm $^{-3}$

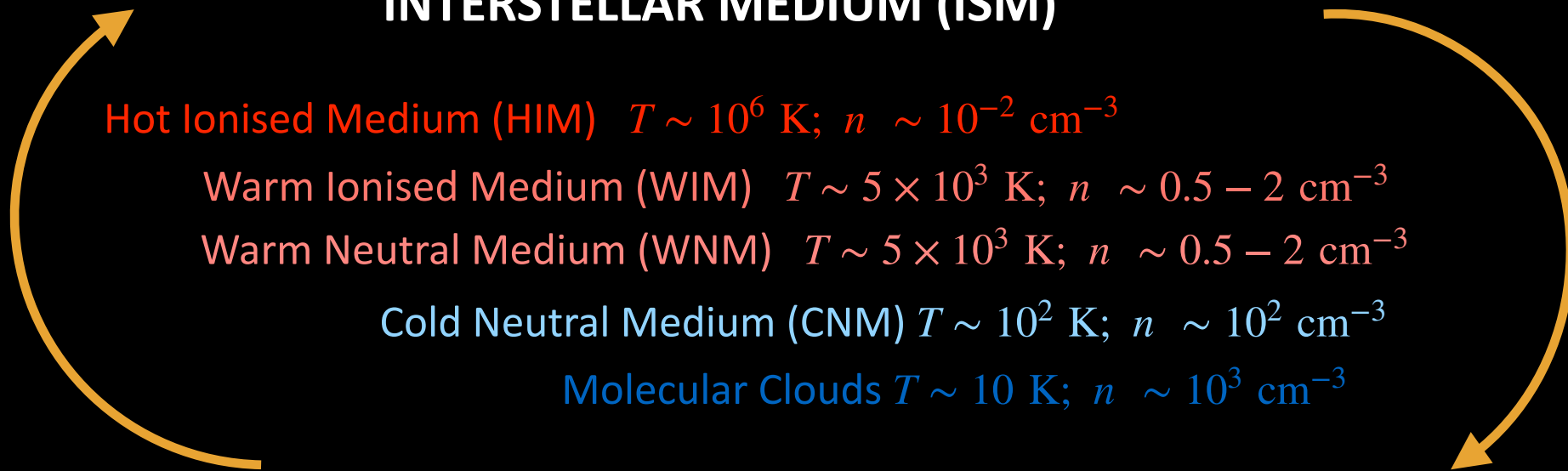
Molecular Clouds $T \sim 10$ K; $n \sim 10^3$ cm $^{-3}$

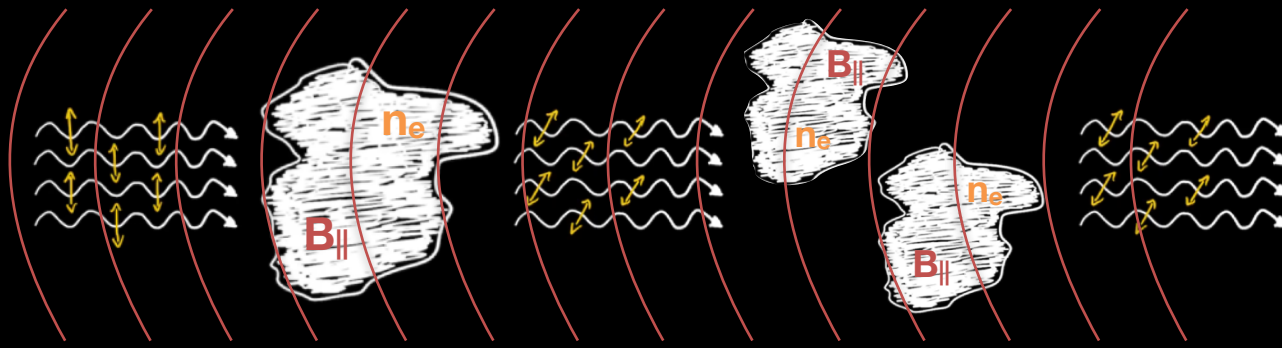
cosmic - rays

cosmic - rays

cosmic - rays

cosmic - rays





	CNM	WNM	WIM	HIM
T [K]	80	5 000	8 000	10^6
n_{H} [cm^{-3}]	30	0.4	0.2	0.005
n_{e} [cm^{-3}]	0.02	0.01	0.2	0.006
L [pc]	10	30	30	100

$B_{\parallel} = 1 \mu\text{G}$ 0.2 rad m⁻² 0.25 rad m⁻² **5 rad m⁻²** 0.5 rad m⁻²

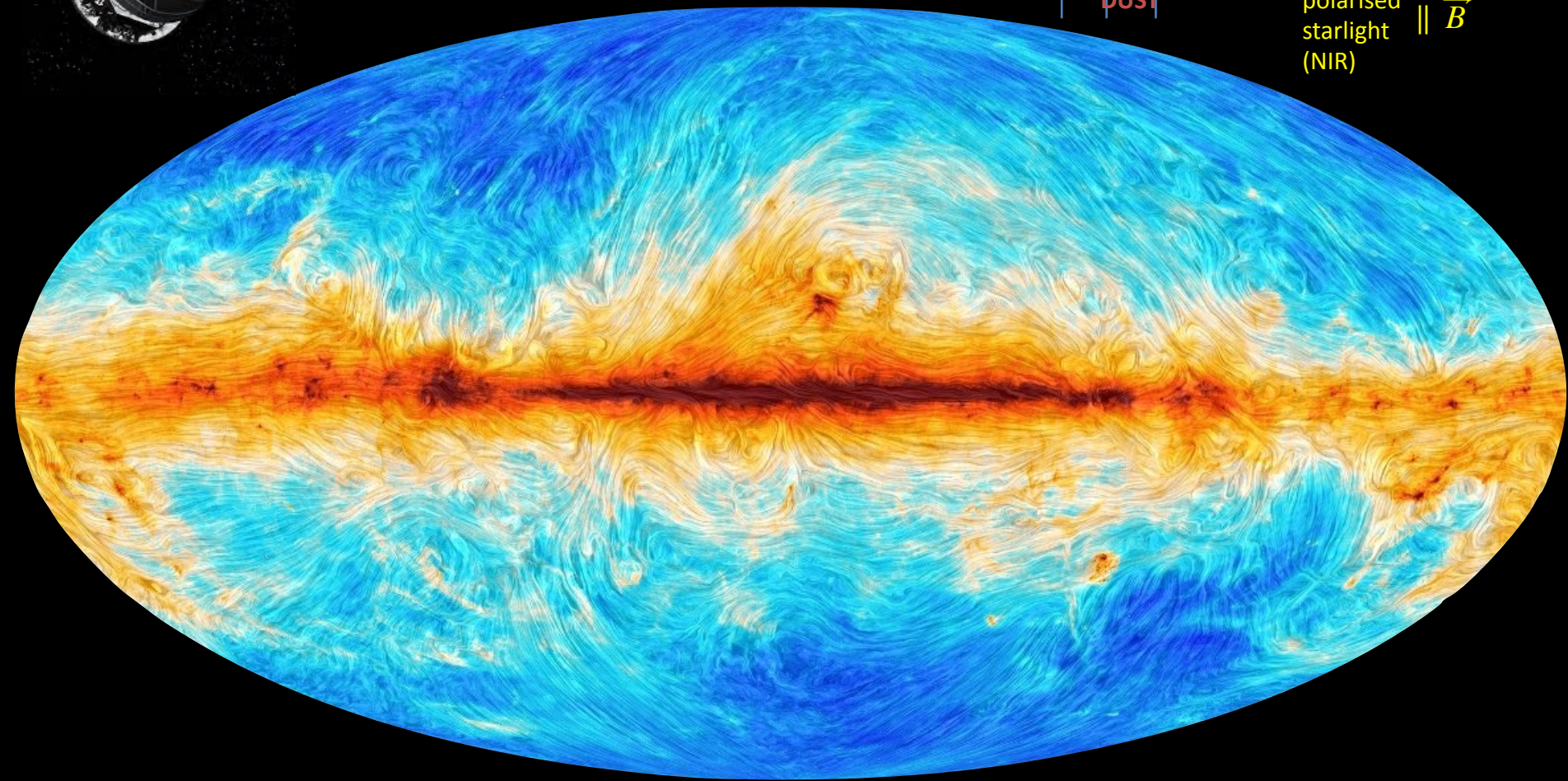
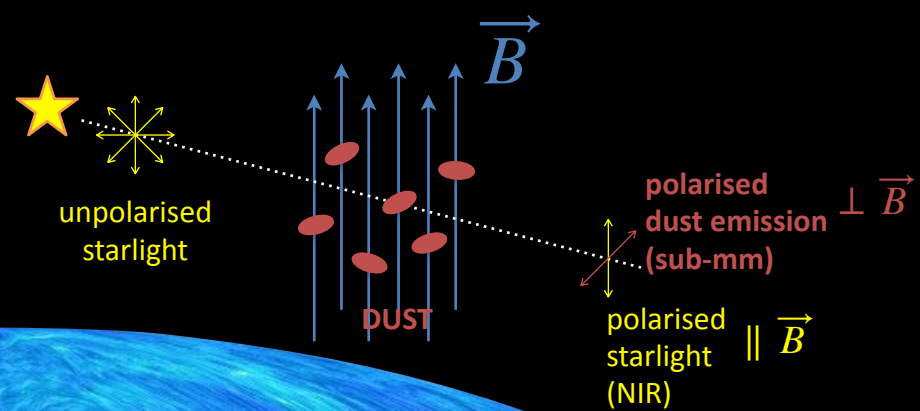
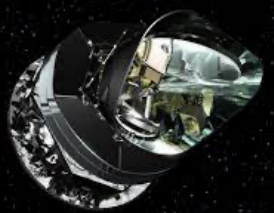
Ferrière 2020

MULTI-TRACERS ANALYSIS + SIMULATIONS

*Zaroubi et al. 2015, Kalberla & Kerp 2016, Van Eck et al. 2017,
Jelić et al. 2018, Bracco et al. 2020, Turić et al. 2021*

Padovani et al. 2021, Bracco et al. 2022

Dust polarized emission

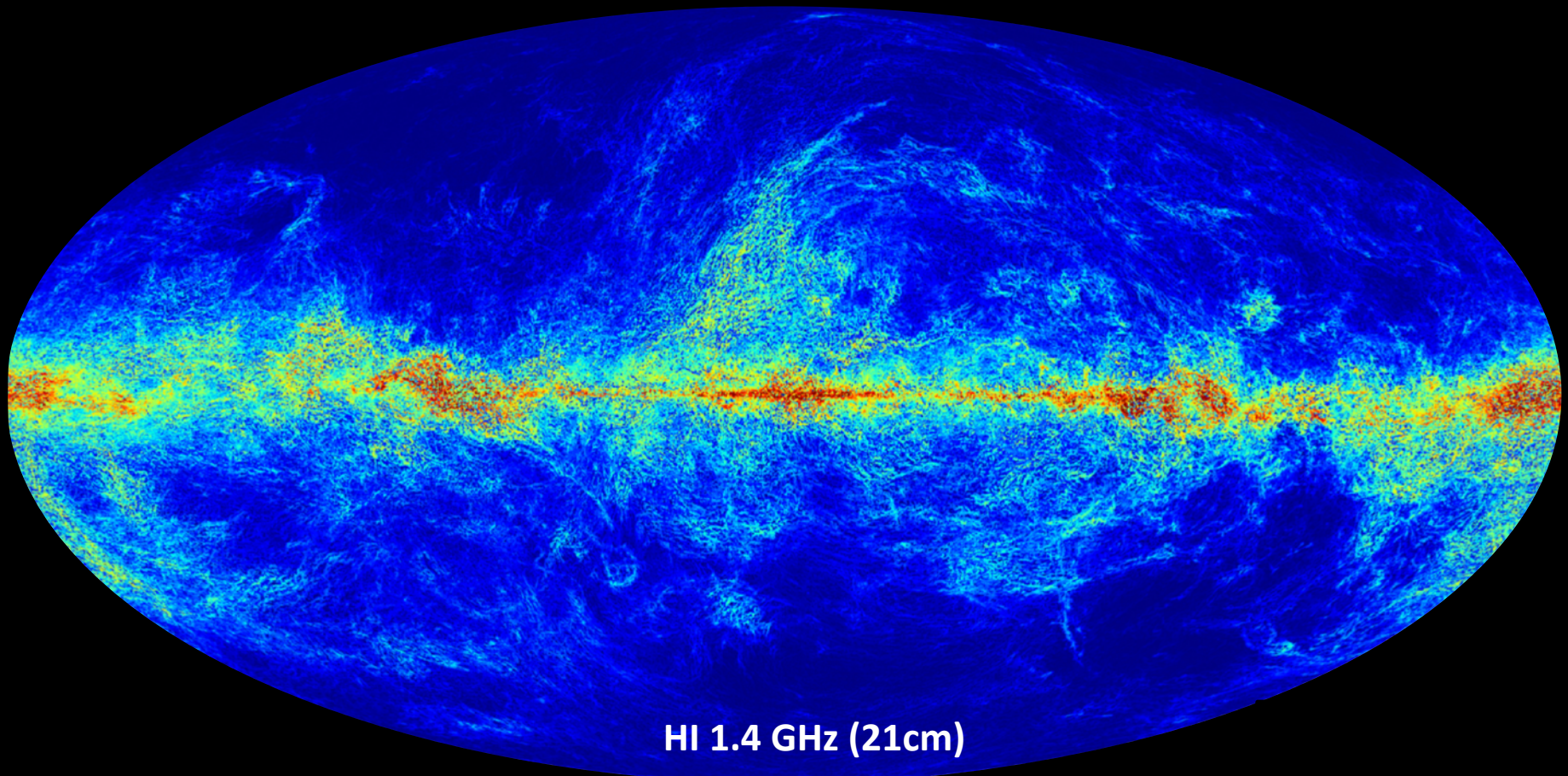


Planck map @ 343 GHz

Planck Collaboration I and XIX 2015

HI emission (GASS, GALFA-HI i EBHIS)

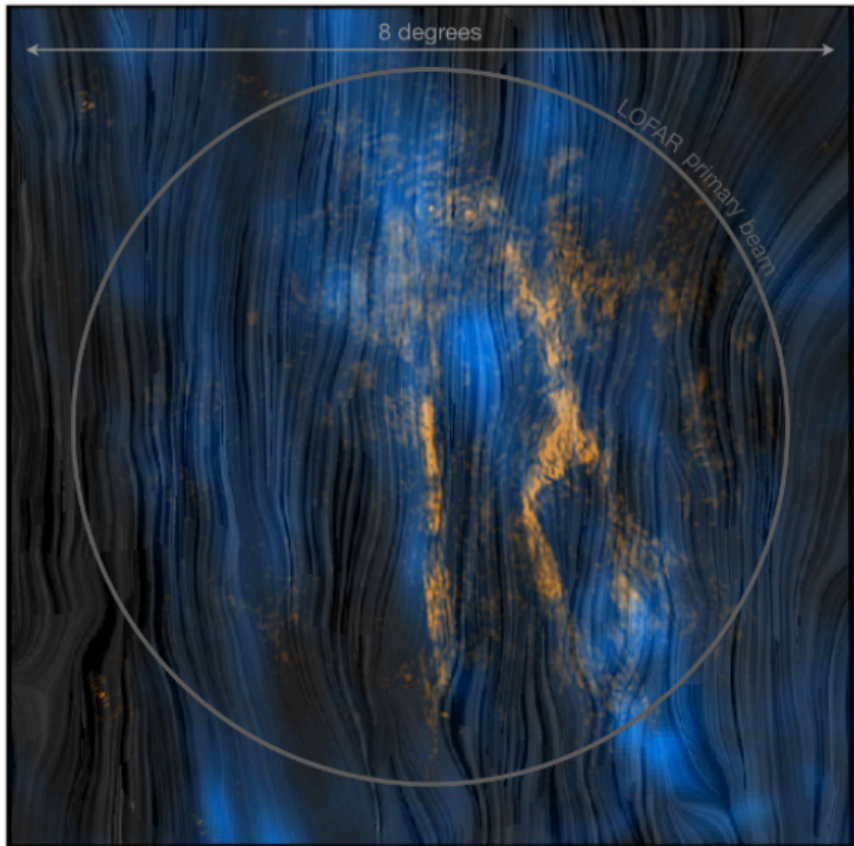
- HI filaments follow orientation of the magnetic field



Clark et al. 2014; Kalberla et al. 2016

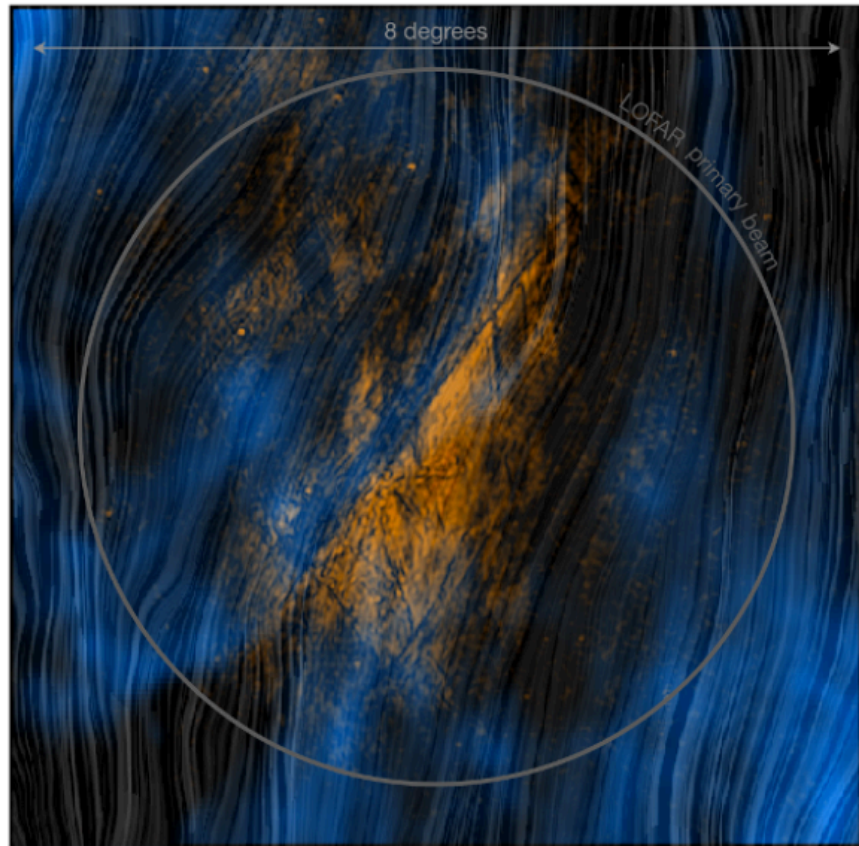
3C 196 field

LOFAR 0 rad/m², EBHIS -5 km/s



Field A

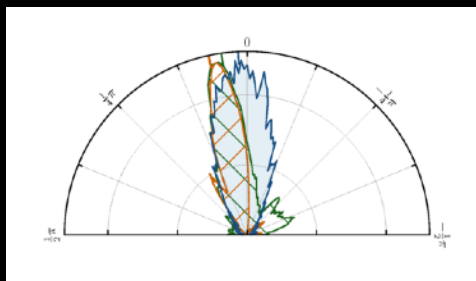
LOFAR -1.25 rad/m², EBHIS +1.4 km/s



Zaroubi, Jelić et al. 2015, Kalberla & Kerp 2016,
Bracco et al. 2020

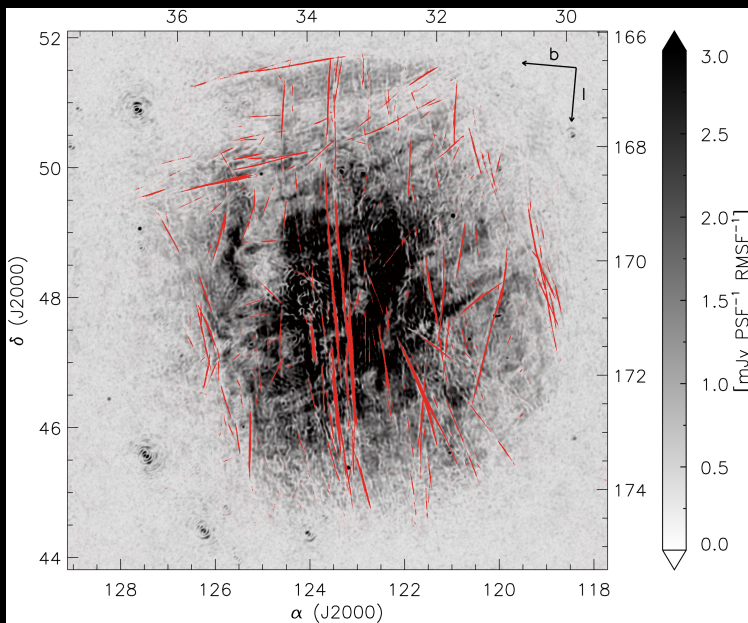
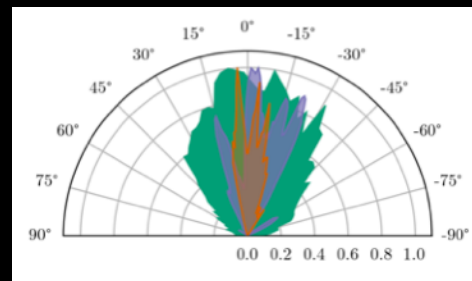
- observed correlation between Faraday structures, magnetic field probed by polarised dust emission and neutral hydrogen (mostly CNM and LNM)

3C 196 field

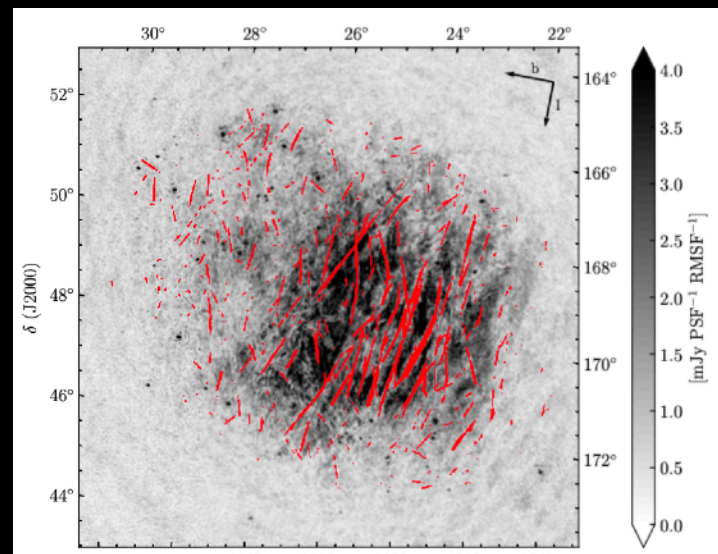


LOFAR data
EBHIS data
Planck data

Field A



Jelić et al. 2018

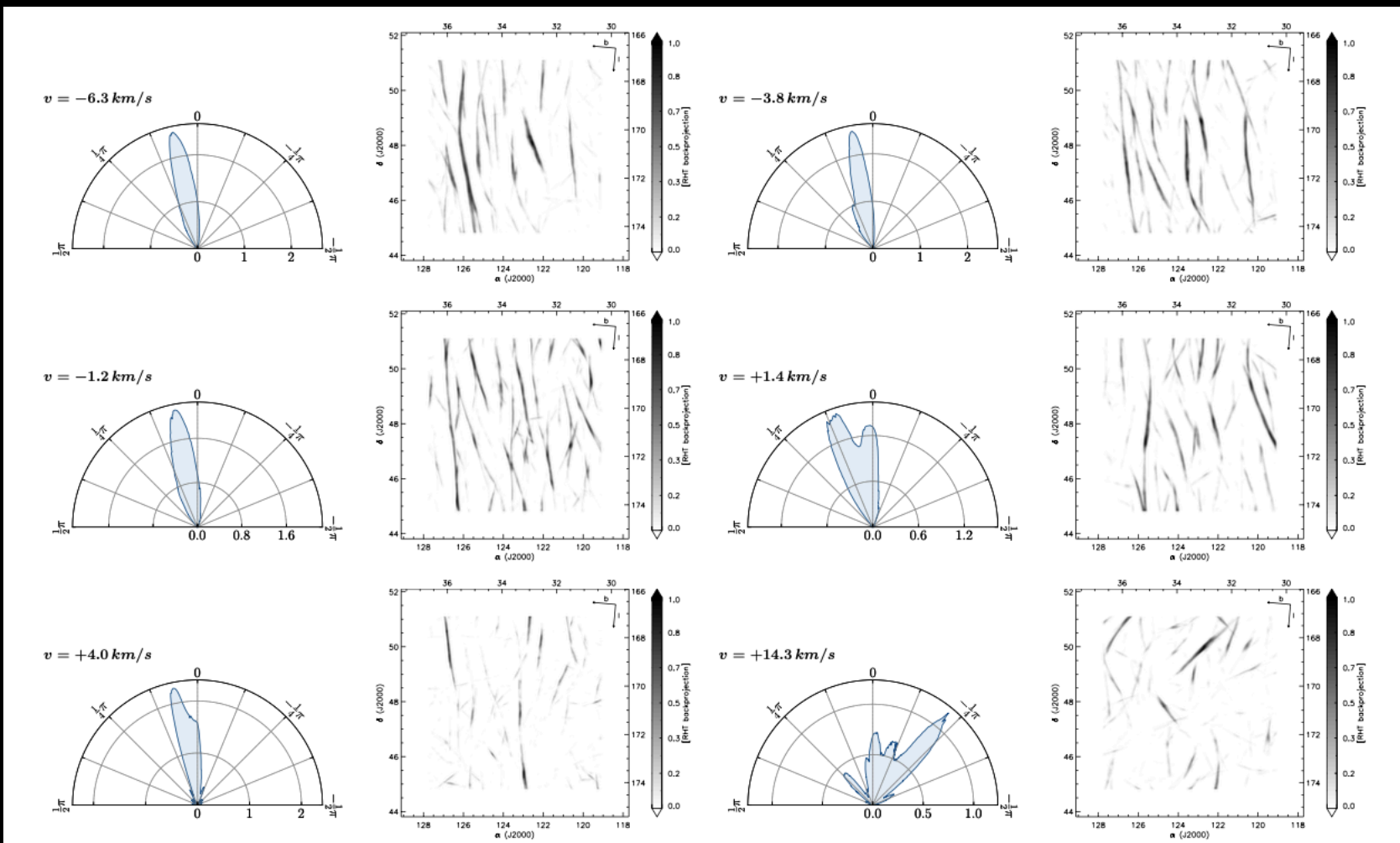


Turić et al. 2021

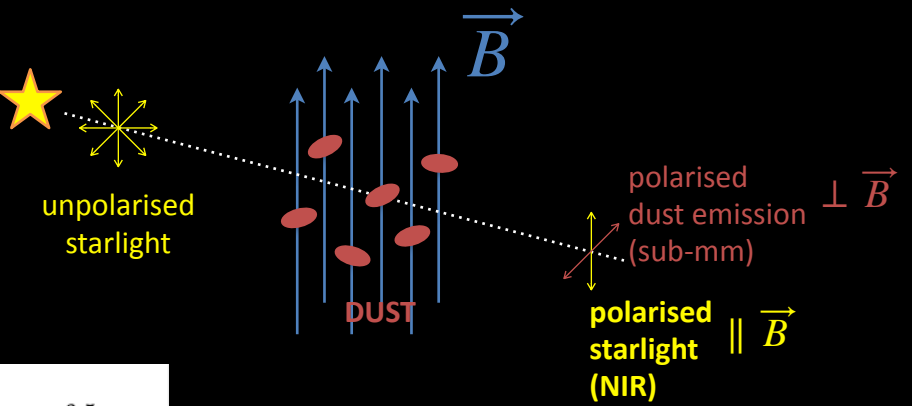
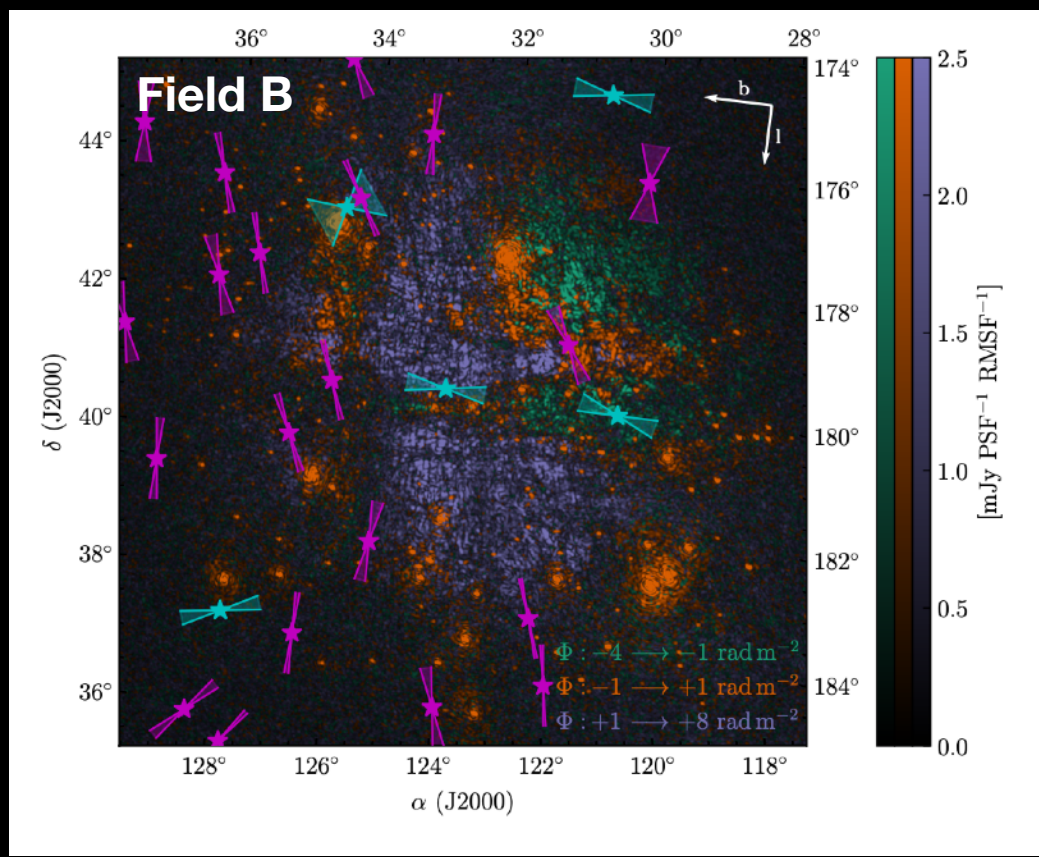
- analysis of straight depolarisation canals using Rolling Hough Transform (**RHT**, Clark et al. 2014)
- *an alignment between three tracers of the local interstellar medium, driven by a very ordered local magnetic field in the plane-of-the-sky*

3C 196 field: HI filaments (EBHIS data)

Jelić et al. 2018

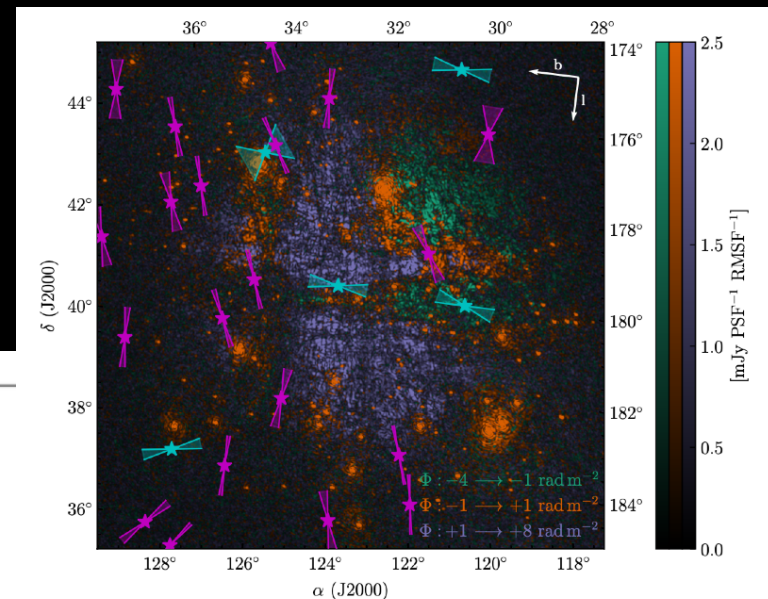
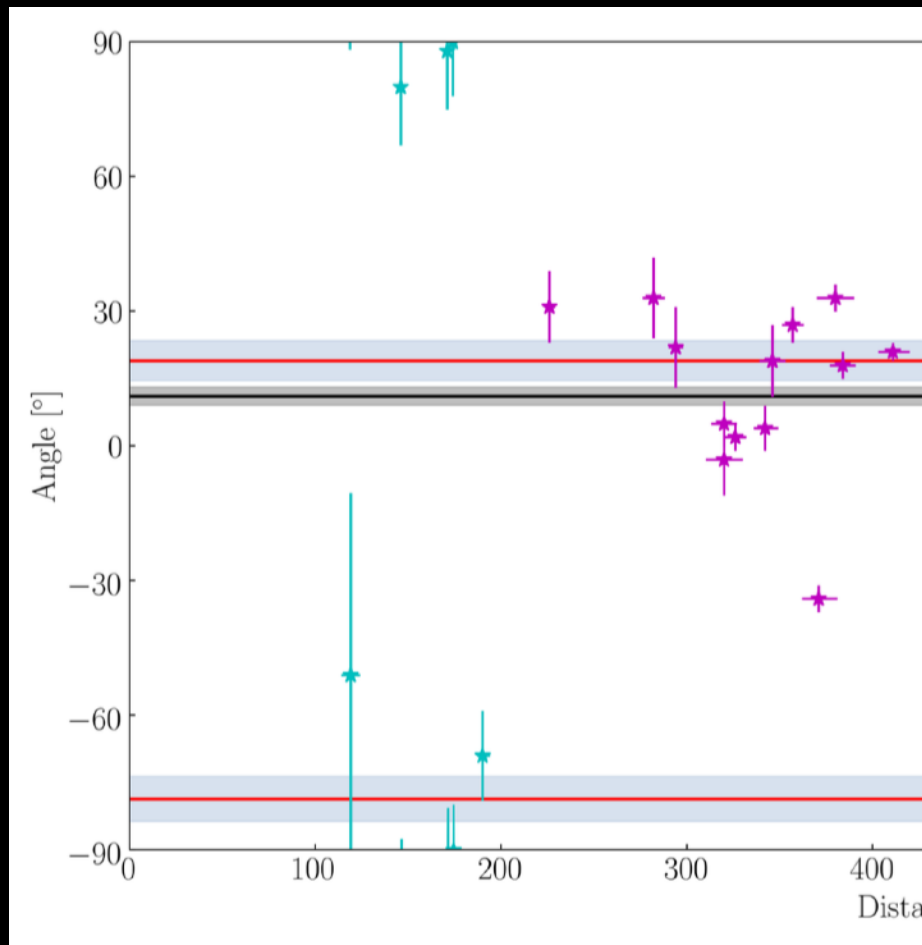


- magnetic field is **coherent** over some parts of the line-of-sight, supported by observations of HI filaments which are aligned to each other over the wide range of velocities (Jelić et al. 2018)
- magnetic field is **tangled** along the line-of-sight, supported by different orientation of HI filaments at different velocities (Clark 2018, 2019)



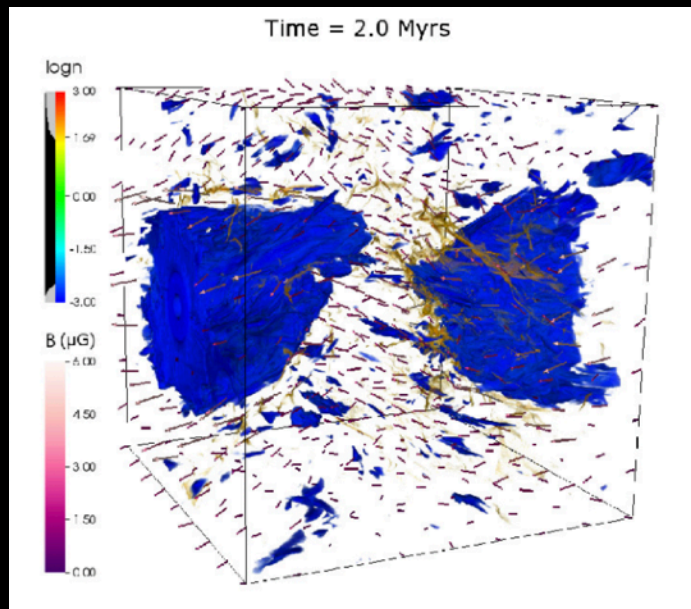
- available starlight polarization data (*Heiles 2000; Berdyugin, A. et al. 2001; Berdyugin, A. & Teerikorpi, P. 2002; Bailey et al. 2010; Berdyugin, A. et al. 2014*) with their distances from the Bailer-Jones catalogue (*Bailer-Jones et al. 2018*), which is based on Gaia Data Release 2 (*Gaia Collaboration et al. 2018*)

- polarized synchrotron emission observed at different Faraday depths originates from different distances:
 - 100 - 200 pc ($-4 \rightarrow 0$ rad/m 2)
 - 250 - 800 pc ($0 \rightarrow +8$ rad/m 2)

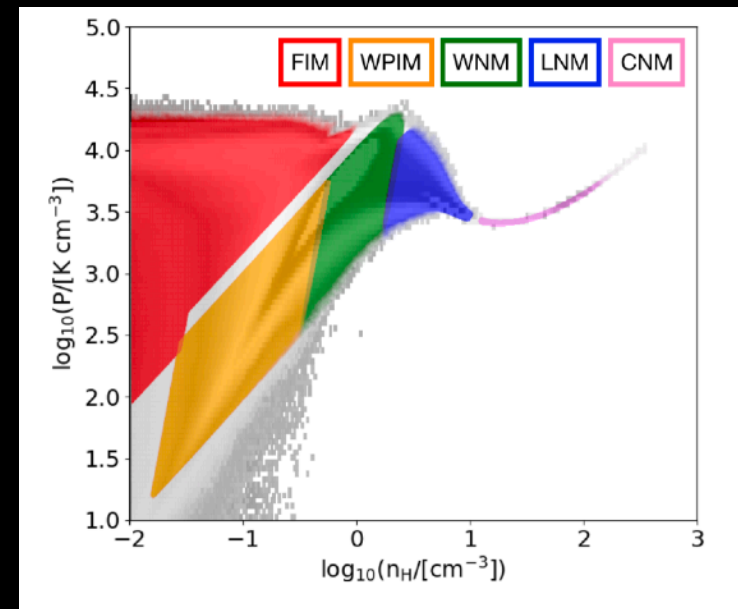


Synthetic observations of the multiphase interstellar medium

- based on *Ntormousi, et al. 2017* MHD simulations of colliding super-shells
- polarized emission from synchrotron radiation based on *Padovani et al. 2021*, assuming uniform distribution of cosmic-ray electrons, with variable energy spectral index
- analytical approach for ionization steady state, based on *Wolfire 2003, Bellomi et al. 2020*

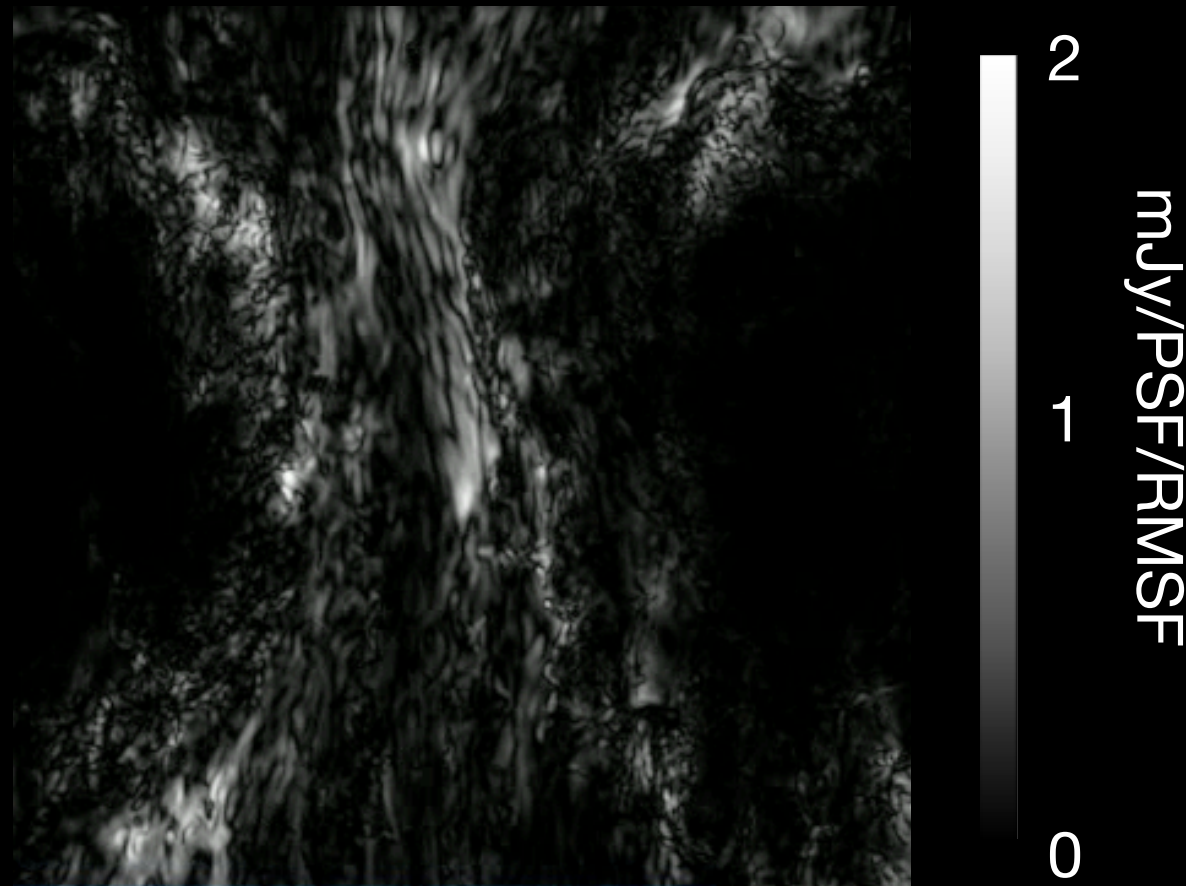


Ntormousi, et al. 2017



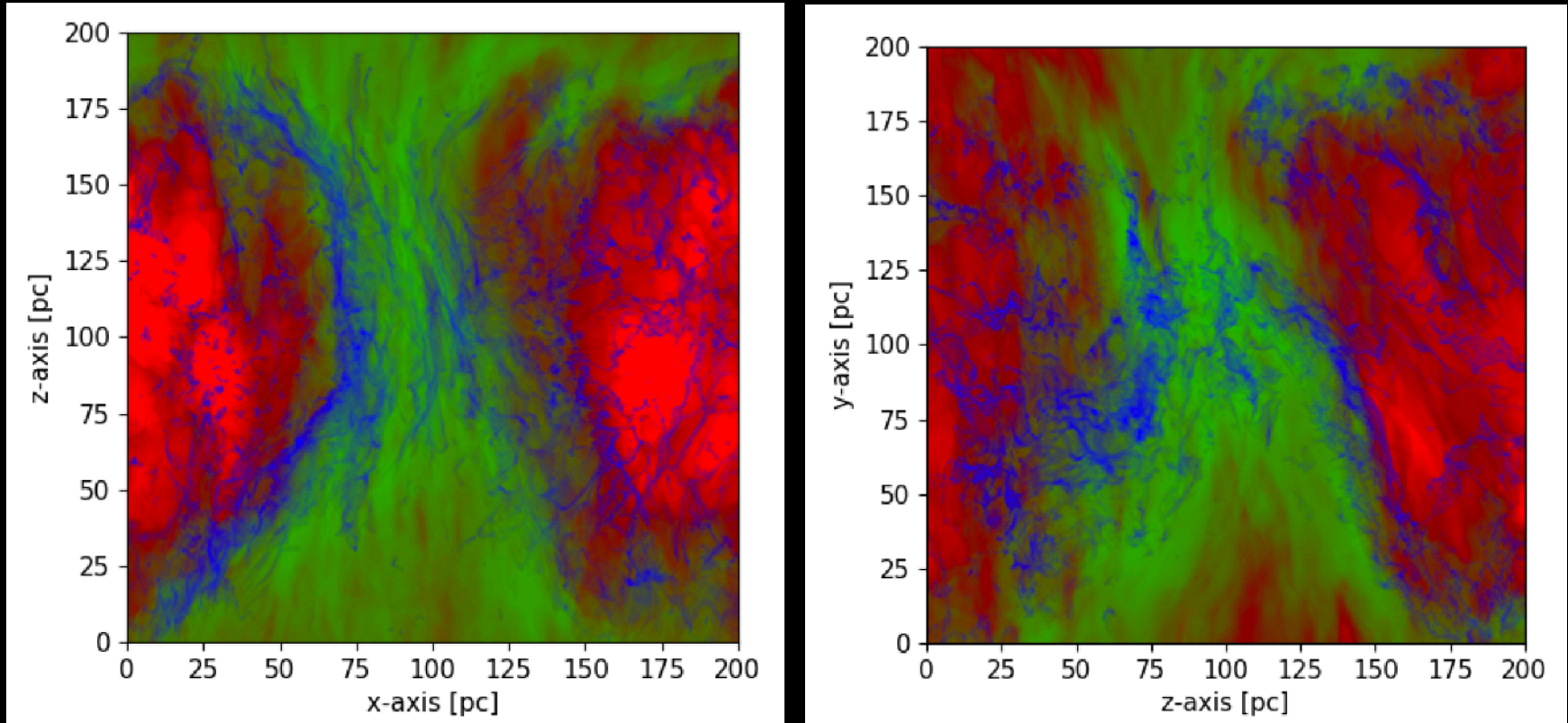
Bracco et al. 2022

Synthetic observations of the multiphase interstellar medium



Synthetic observations of the multiphase interstellar medium

- in the simulations we can distinguish warm/ionized to cold/neutral phases



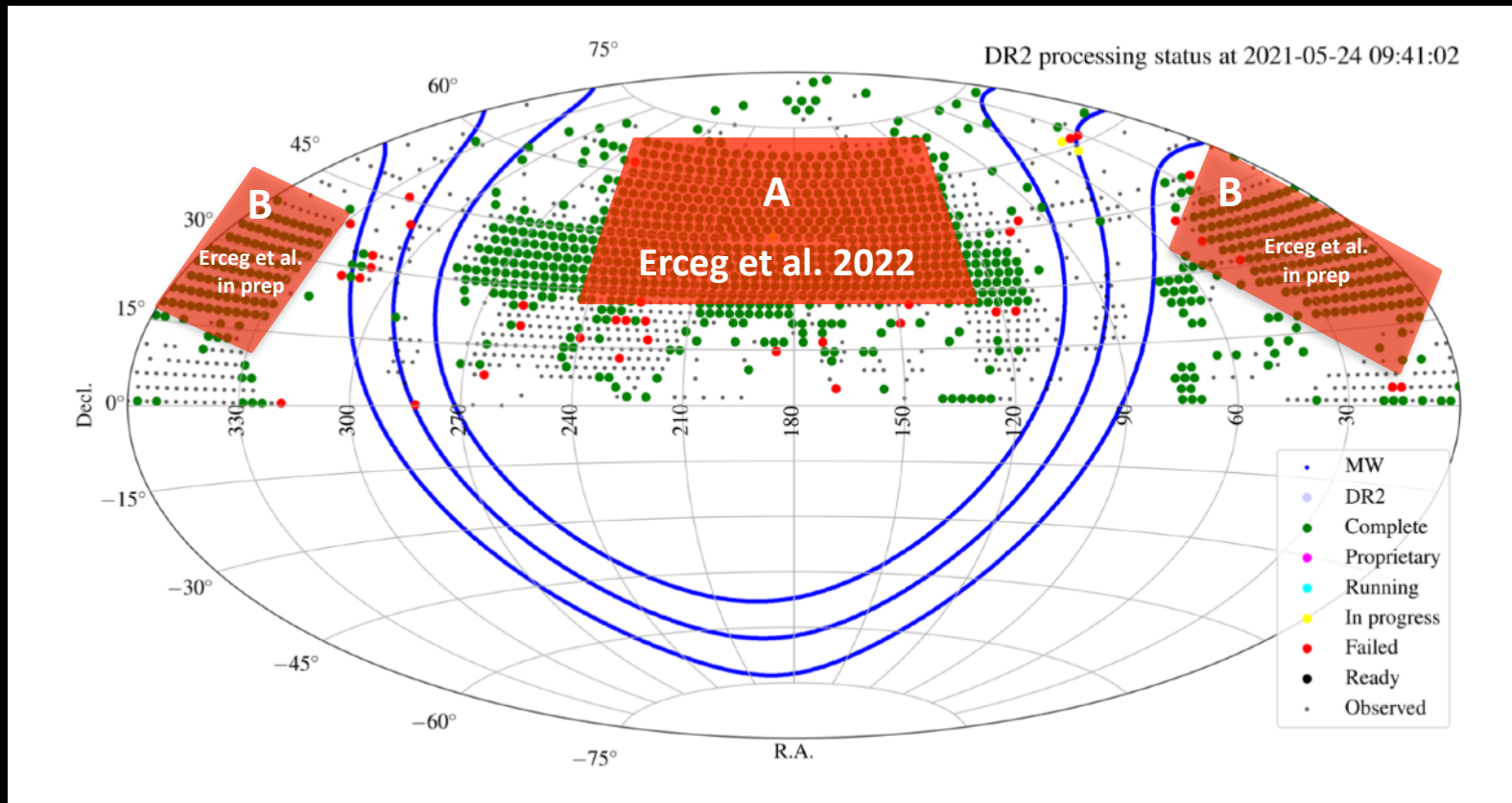
Hot/fully ionized Warm/partially ionized Cold/neutral

- strong correlation is found with warm/partially ionized, where is the cold gas in polarization ?

LoTSS - LOFAR Two-metre Sky Survey

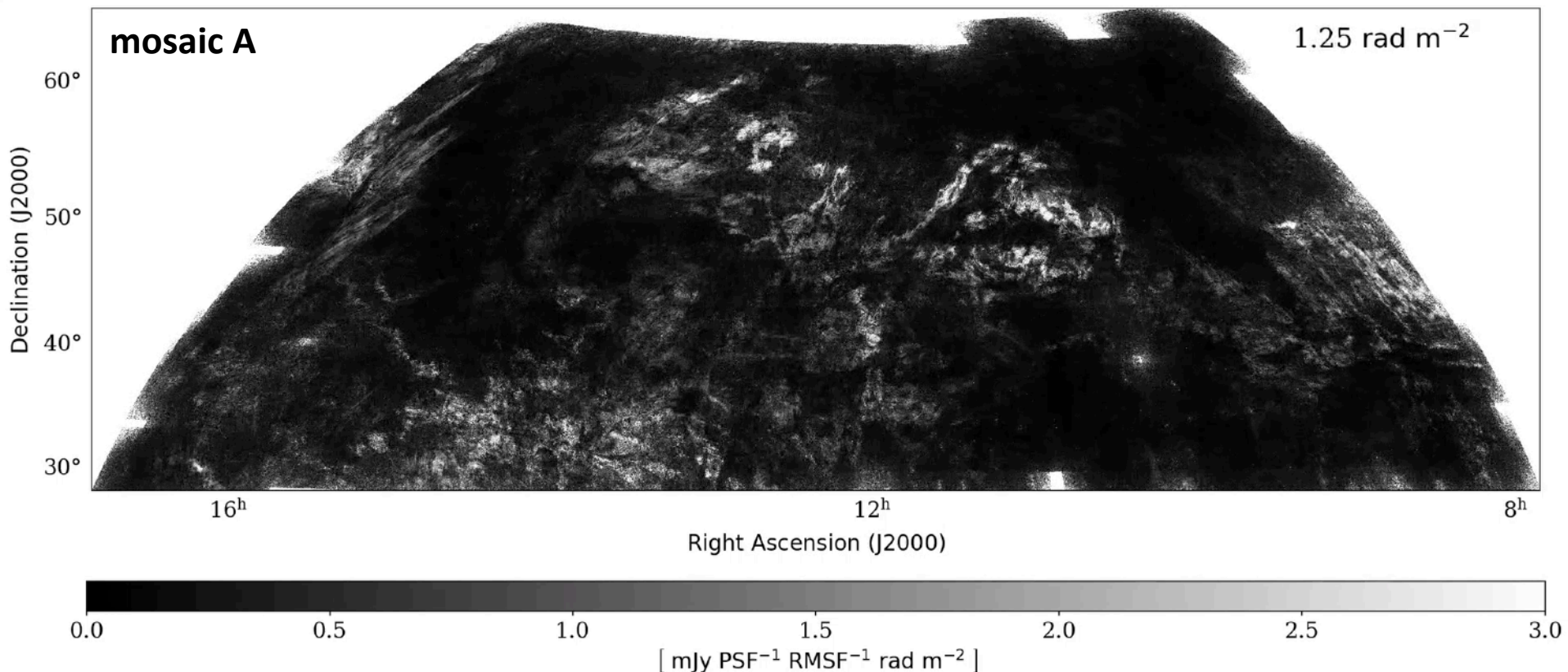
<https://lofar-surveys.org>

Shimwell et al. 2017, 2019, 2022

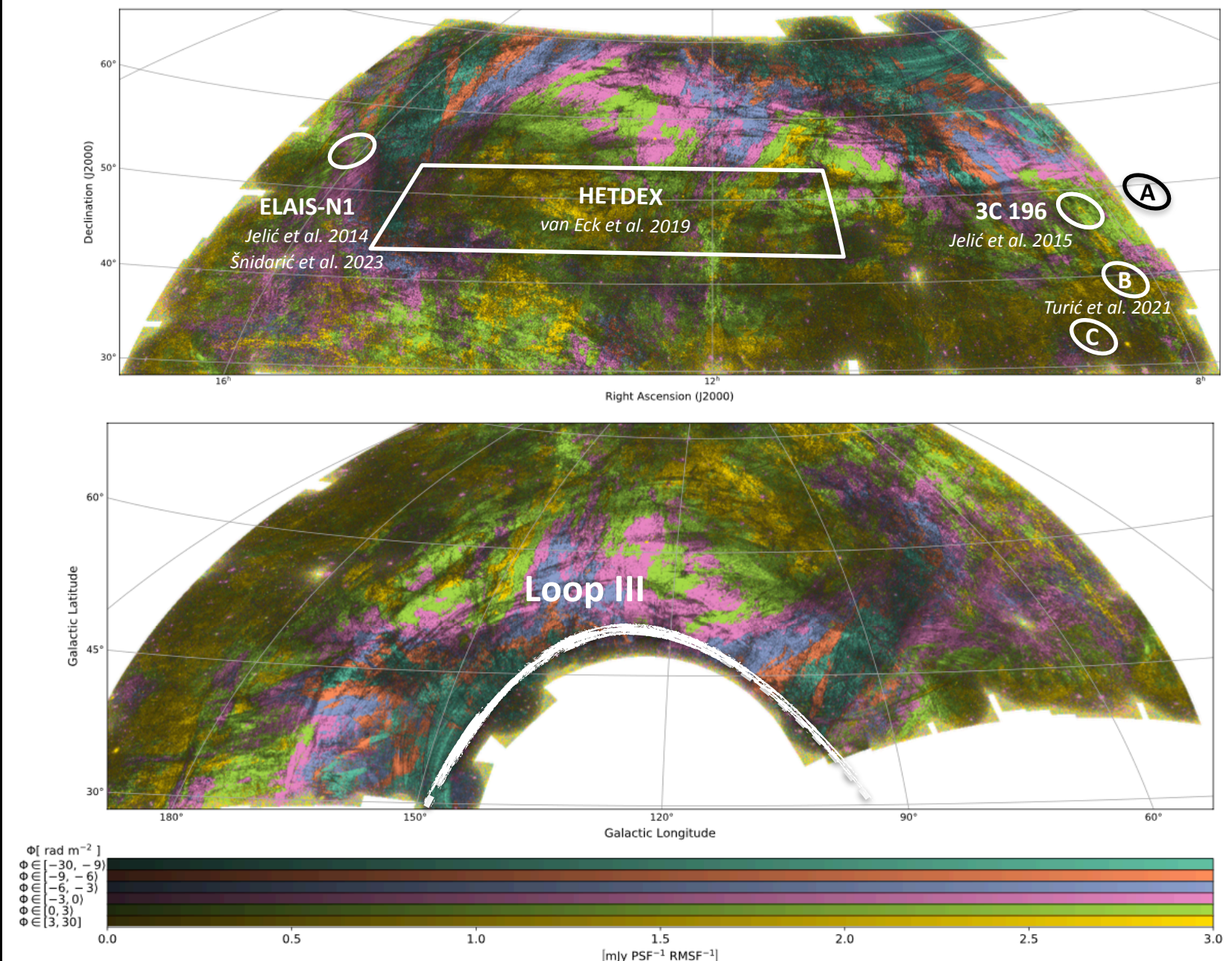


- LOFAR-HBA observations (120 - 168 MHz)
- mosaic A: $841 \times 64 \text{ deg}^2$ fields towards outer Galaxy (3100 deg^2)
- mosaic B: $198 \times 64 \text{ deg}^2$ fields towards inner Galaxy (1200 deg^2)

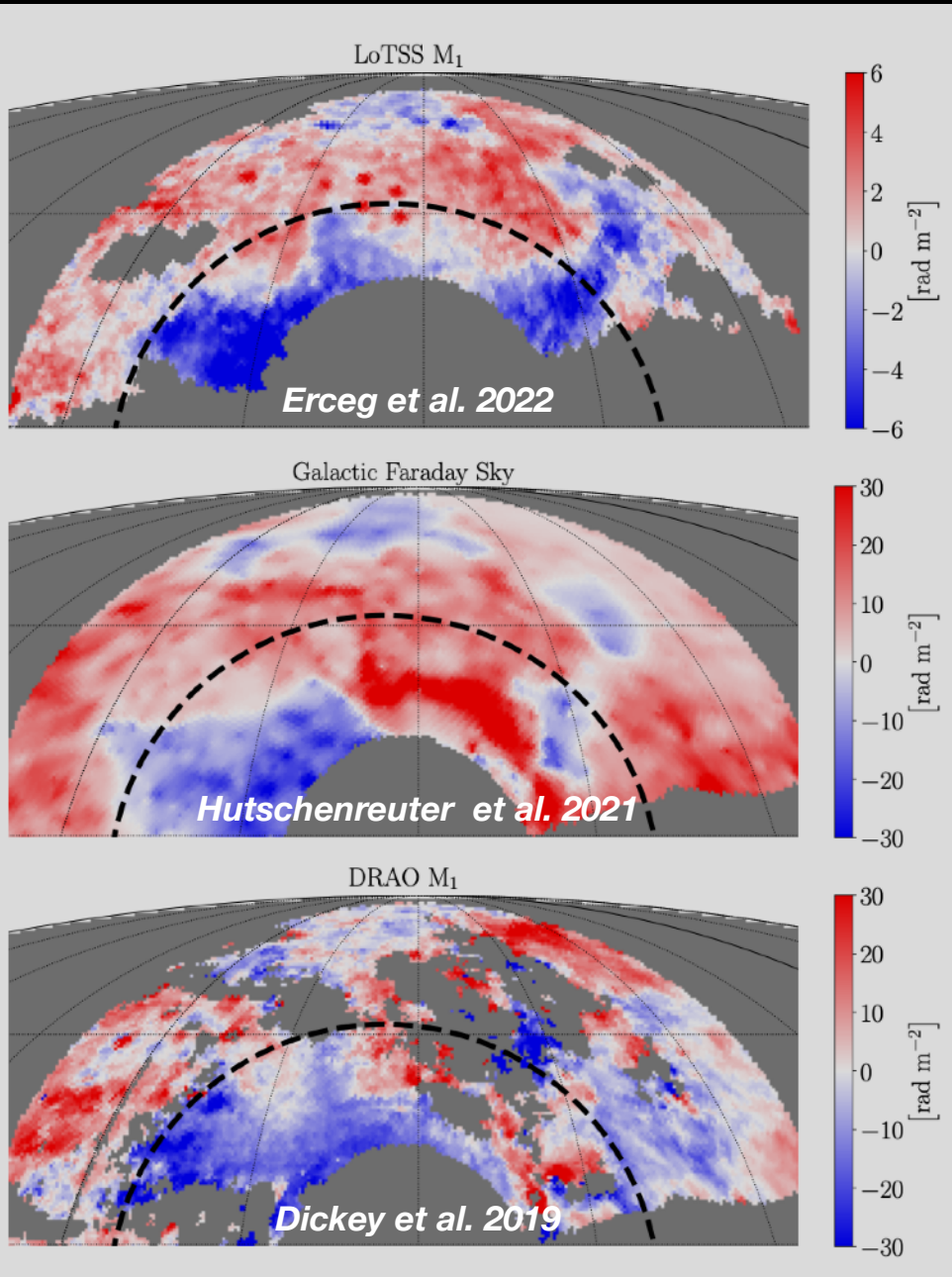
The intermediate Galactic latitude in the outer Galaxy



LoTTS Survey DR2: Erceg et al. 2022



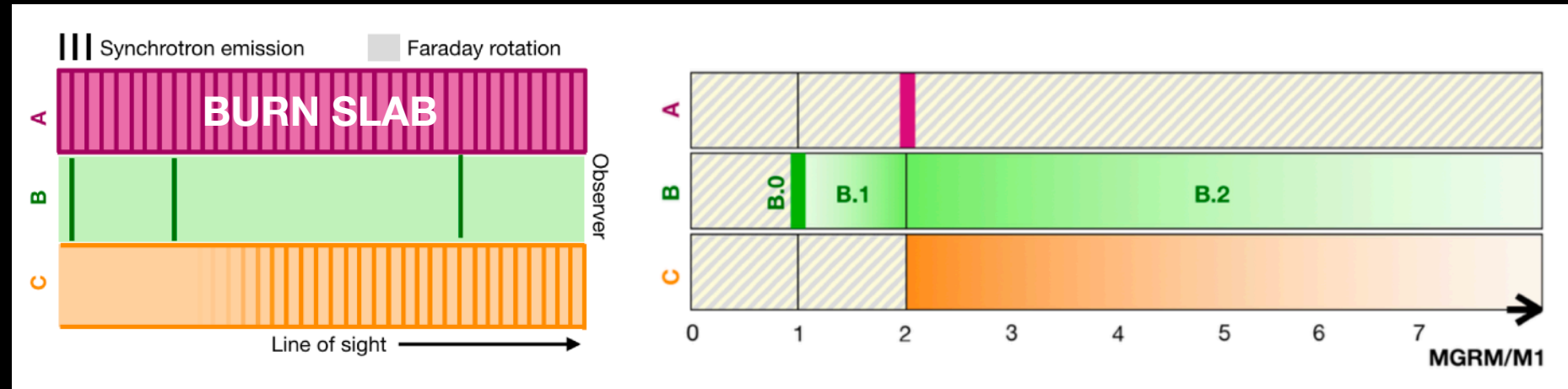
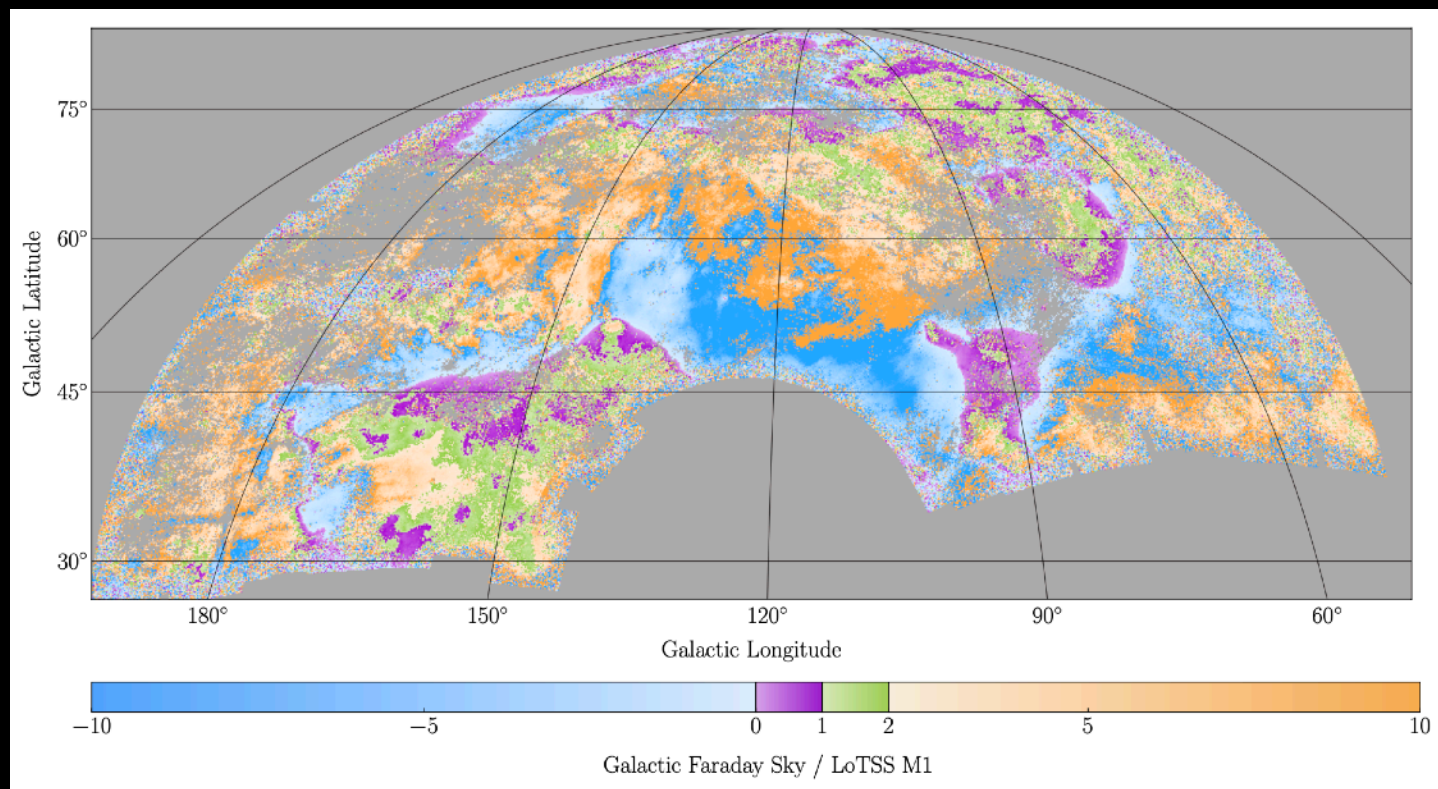
LoTSS Survey DR2: Erceg et al. 2022



M1 - First Faraday moment - intensity weighted mean Faraday depth

Galactic Faraday Sky - the total RM produced by the Galaxy, reconstructed using extragalactic sources

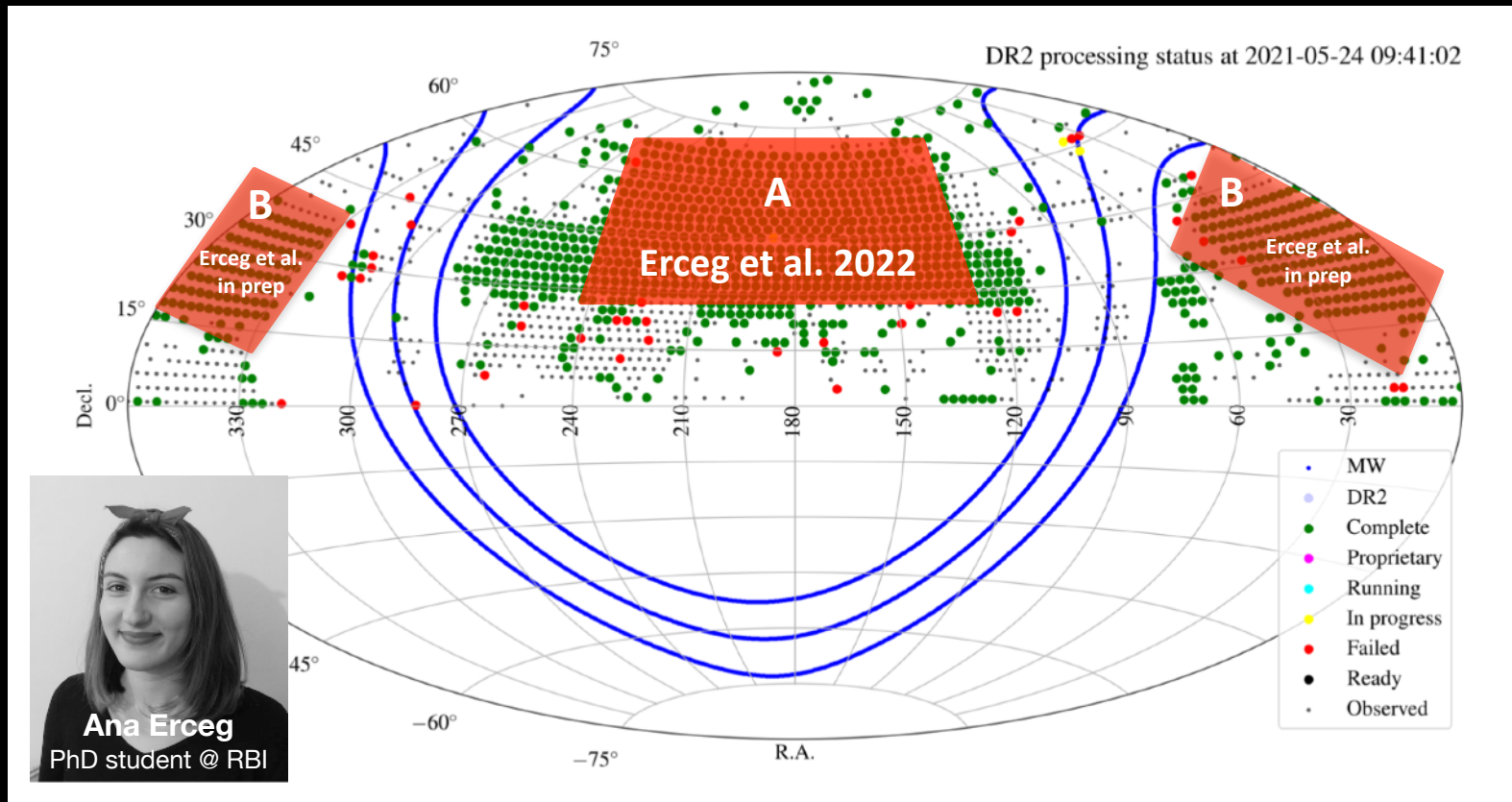
- a correlation between the LoTSS M₁ and the Galactic Faraday Sky
- a lack of correlation between the LoTSS M₁ and DRAO GMIMS M₁ - a result of frequency-dependent Faraday depth resolution and depolarisation



LoTSS - LOFAR Two-metre Sky Survey

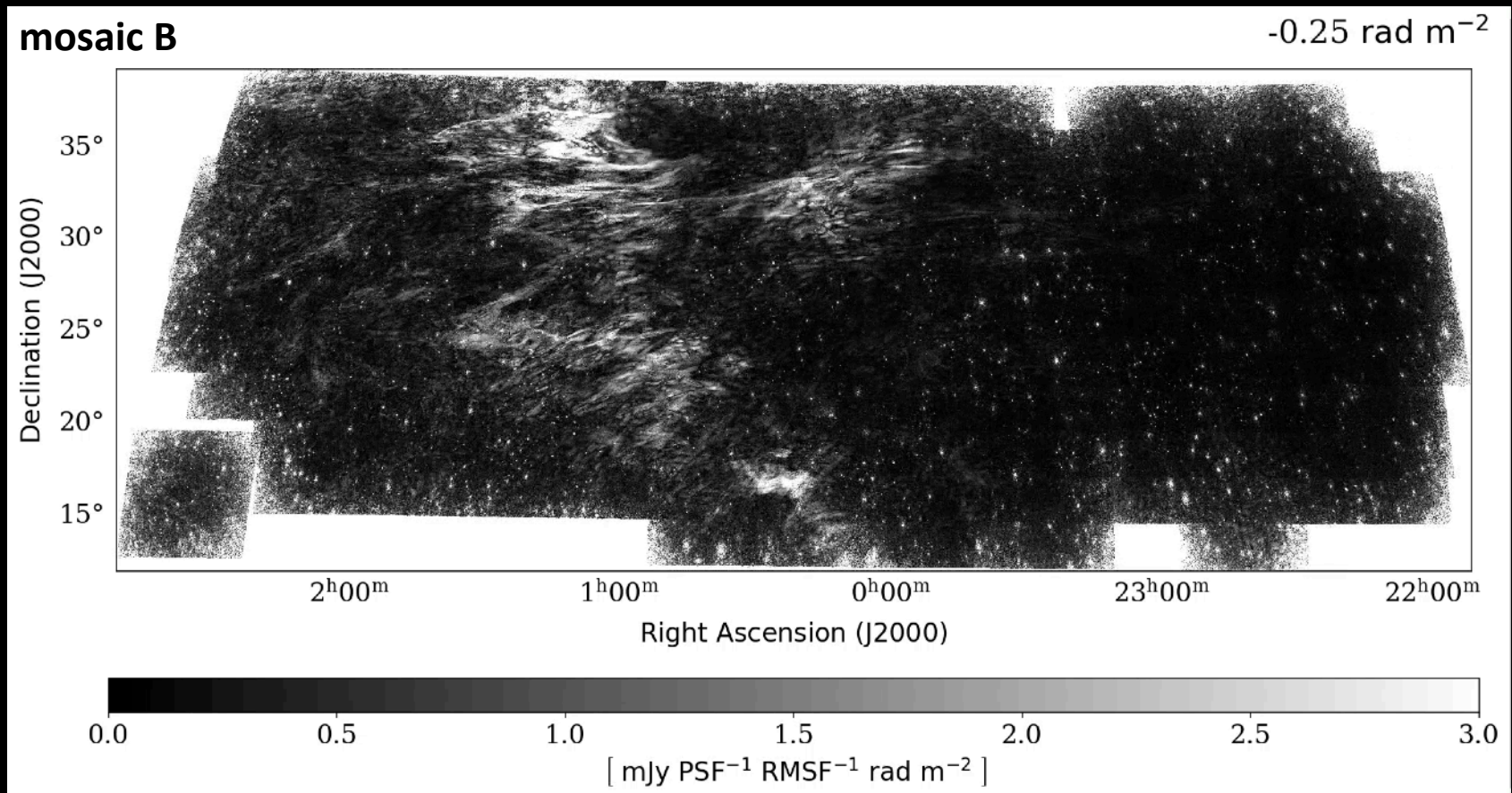
<https://lofar-surveys.org>

Shimwell et al. 2017, 2019, 2022



- LOFAR-HBA observations (120 - 168 MHz)
- mosaic A: $841 \times 64 \text{ deg}^2$ fields towards outer Galaxy (3100 deg^2)
- mosaic B: $198 \times 64 \text{ deg}^2$ fields towards inner Galaxy (1200 deg^2)

The intermediate Galactic latitude in the inner Galaxy



LoTTS Survey DR2: Erceg *et al.* *in prep.*

- LOFAR (115 - 175 MHZ) is an excellent instrument to do Faraday tomography of the local ISM and constrain its physical properties
- morphology of the observed polarized emission is very rich, with the brightness temperature up to tens of K, including a discovery of many filamentary structures and linear depolarization canals
- based on multi-frequency/multi-tracers analysis we found an alignment between three distinct tracers of the local ISM, the ordered magnetic field plays a crucial role in confining different interstellar medium phases
- the spatial distribution of the LOFAR polarization as a function of the distance can be studied by using the state-of-the-art starlight extinction and polarization data